VOL. 1 No. 3 MARCH 1936

Philips Technical Review

DEALING WITH TECHNICAL PROBLEMS
RELATING TO THE PRODUCTS, PROCESSES AND INVESTIGATIONS OF
N.V. PHILIPS' GLOEILAMPENFABRIEKEN

EDITED BY THE RESEARCH LABORATORY OF N.V. PHILIPS' GLOEILAMPENFABRIEKEN, EINDHOVEN, HOLLAND

# A NEW METAL RECTIFYING VALVE WITH MERCURY CATHODE

By J. G. W. MULDER.

**Summary.** The new type of rectifying valve with mercury cathode described in this article has a cathode chamber which is made of metal and is water-cooled. Owing to the use of chrome-steel the pump which has hitherto been necessary with metal rectifier chambers has been dispensed with. The valve is of the single-phase type, whereby its construction has been much simplified and at the same time its dimensions considerably reduced. The new type of rectifier is designed for medium and high powers corresponding to current intensities of about 50 to several hundred amps per unit.

## Introduction

For the rectification of high powers, rectifying valves with a mercury cathode ¹) are particularly suitable, owing inter alia to their ability to withstand overloading. The development of these rectifying valves has resulted in the production of two main types, the glass valve and the metal valve.

Where high powers have to be rectified the main difficulty in the design of rectifying valves, as in many other branches of electrical technology, has been the dissipation of the heat generated. This problem is dealt with by introducing a system of artificial cooling, a current of water being the most efficient. Water cooling is most suitably carried out with a metal valve body and has led to the construction of mercury cathode rectifiers with iron jackets for currents above 1000 amps, which are equipped with a water-cooling system and a high-vacuum pump. The latter was essential in this class of rectifier, as hydrogen ions present in the water diffuse through the iron walls. But the need for high-vacuum pumps in order to employ water cooling had many disabilities, since the presence of the pump, in spite of the use of automatic regulating devices, called for more careful supervision of these rectifiers than was required with sealed rectifier valves.

For this and other reasons metal rectifier valves were not constructed for currents below 1000 amps. In the glass valves which were used for these ratings, the dimensions had to be very large in order to provide for the necessary dissipation of the heat generated. But there is naturally an upper limit in dimensions to which glass bulbs can be manufactured. So that if with the maximum practical dimensions the valve was still unable to dissipate all the heat generated, it became imperative to adopt more intensive air cooling.

At the Philips Works a new type of metal single-phase rectifying valve with mercury cathode has now been evolved which, like glass valves, is used in a sealed condition. In this valve which is intended for a power range at

---

¹) This term appears to us more suitable than that in common use hitherto, viz, "mercury rectifying valve", as thermionic rectifying valves nowadays also frequently contain an atmosphere of mercury vapour.

present catered for by glass mercury-cathode rectifying valves (and even for still higher powers) the same advantages are offered as by the iron types rated for high powers, while the pump necessary in the latter has been dispended with in the new rectifiers. This new type of rectifying valve is described in the present paper [2]).

### Construction of the New Type of Valve

A diagrammatic section through the valve is shown in *fig. 1*. The cathode is a pool of mercury *K* contained in a chrome-steel chamber. The latter is cooled by a current of water which circulates between the wall of the valve and a metal cooler which is screwed on to the outside for this purpose. The use of chrome-steel enables the valve to be sealed without raising any difficulties regarding the maintenance of a vacuum, since no hydrogen diffuses through chrome-steel into the valve as was known in this laboratory from the experience with water-cooled transmitting valves. The general design is, however, here the exact reverse to that adopted with transmitting valves, for in the latter the chamber acts as the anode, while here it is the cathode. The chamber is pressed from a single piece of sheet metal.

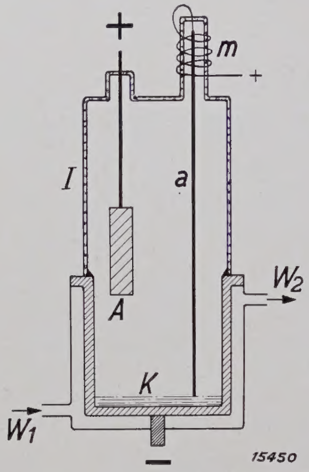

Fig. 1. Section through new type of mercury-cathode rectifying valve (schematic). The cathode *K* is a pool of mercury in a chrome-steel chamber, and the anode *A* a graphite block. The chrome-steel chamber and the glass anode insulator *I* form a hermetic seal. The chamber is cooled with water which flows in at $W_1$ and flows out at $W_2$. An auxiliary anode *a* with a magnetising coil *m* provides ignition.

A partition has been fitted inside the cooler to avoid water remaining at rest in "dead" ends. The chamber is as a result uniformly and effectively cooled, and the greater part of the discharge takes place in this highly-cooled metal system.

The glass anode insulator *I* forms a hermetic seal with the edge of the cathode chamber. The head of the cathode insulator with the two cylinders mounted on it is pressed in one piece. The two welded joints are produced by machine.

The anode *A* is a graphite block. The valve is started in the usual way by an auxiliary anode *a*, which can be moved up and down through a short distance. At the beginning an auxiliary direct current which has been rectified independently flows through the auxiliary anode and a magnetising coil *m* connected in series with it, which then draws the auxiliary anode out of the mercury. The arc generated in this way ignites the actual discharge.

The temperature of the anode insulator *I* must be kept below a specific maximum in order to avoid damage, while on the other hand it must not fall below a certain minimum in order to prevent mercury condensing on the inner wall during the running of the valve. All mercury which is volatilised from the cathode spot must become deposited on the metal walls before it can reach the anode; if there is mercury on the anode back-firing may occur.

The design of valve shown in fig. 1 is suitable for low voltages. For higher voltages special cooling and de-ionisation walls must be introduced in the usual way in the discharge path of the valve. One or more of these walls may be suitably insulated and then act as a control grid. In their place, however, the auxiliary anode *a* can also be replaced by an ignition unit permitting the ignition time to be displaced, as required, with respect to the phase of the anode voltage.

The complete valve mounted in its cooler is shown in *fig. 2*.

### Single-phase or Polyphase Valves

Hitherto rectifying valves with mercury cathodes have always been of polyphase construction, i.e. with an anode for each phase of the polyphase alternating current and a single common cathode for all phases. There are various reasons for this policy. In the first place the polyphase mercury-cathode rectifying valve is more stable in service, as the anodes assist each other when starting up. The generation and maintenance of the cathode spot is indeed the weakness in all designs of this type of rectifier [3]). Secondly, in a polyphase valve a single common auxiliary ignition-system can be used for starting up in all phases. This system consists of an ignition anode and two auxiliary anodes for which an auxiliary current of several amps is independently rectified and smoothed. There is still another important reason for building mercury-cathode rectifying valves always on the polyphase principle. Each valve must, even if it were built on single-phase lines, be provided with a spacious condensing chamber for the purpose of condensing so much of the mercury volatilised that the pressure in front of the anodes remains low. In a polyphase design this domed chamber, which at any rate must be provided, is employed far more efficiently.

---

[2]) In the design and testing of the new valve, valuable assistance was rendered by Mr. Lems.

[3]) Thermionic rectifiers are certainly more convenient in this connection, where the heated cathode is always ready for emitting electrons. Directly-heated or indirectly-heated hot-cathodes for emission currents of several hundred amps are indeed feasible, but introduce a number of practical difficulties.

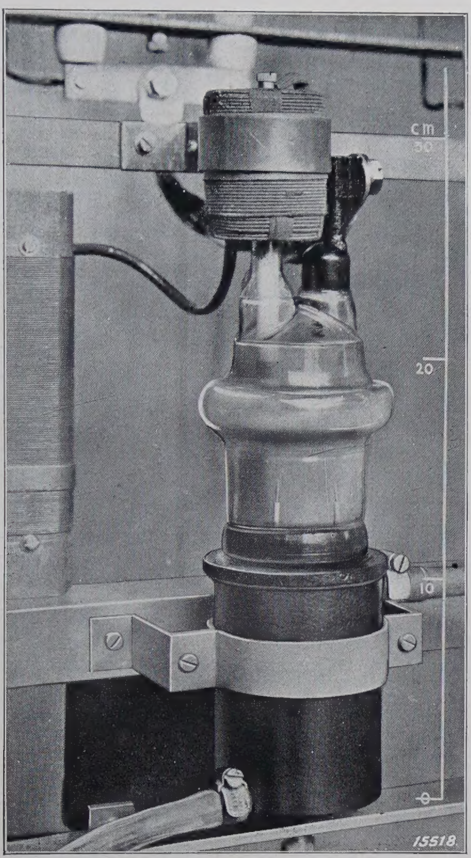

Fig. 2. Construction of the single-phase metal rectifying valve shown diagrammatically in fig. 2.

In the new type of valve this chamber has become superfluous owing to the vigorous cooling action of the metal walls. For this reason a single-phase design is more practical [4]) in the present case. It offers important advantages which more than completely outweigh the above-mentioned drawback that adequate provision for satisfactory ignition must be made for each valve individually. General construction is thus considerably simplified, and permits complete mechanical manufacture, so that six single-phase metal valves are better productions than a single glass valve rated for a sixfold current. The dimensions can be kept small, since in the negative phase no anode is affected by the ionisation produced by the current flowing to one of the other anodes. (This phenomenon would again occasion large dimensions in the case of polyphase valves, so that the advantages due to watercooling would not be entirely utilised. See also footnote [4])). Erection and transport are extremely simple with the single-phase metal valves. In service it is, moreover, important that when using single-phase valves a spare for only a fraction of the total power of the plant need be provided. In addition, the liability to defects which usually occur only at leading-through points and welded joints is still lower with the simple single-phase valves than with one corresponding polyphase valve. Finally, if a valve fails the rectifying plant does not cease operating as a whole since the remaining valves continue to run.

### Characteristics of the New Type of Valve

The valve shown in fig. 2 is rated for a medium current of 75 amps and a peak current of 500 amps. Like other mercury-cathode rectifying valves this valve can without trouble carry heavy overloads for short periods. The only damage which overloads could do would be to produce too high a temperature rise, which, however, requires a certain time. The valve can sustain a 50 per cent overload for 5 minutes and a 100 per cent overload for 30 seconds. The quantity of cooling water required is comparatively low, as on full load only about 1150 watts are converted to heat in the valve. Each valve requires about 1 litre of water per minute, the temperature of the water rising by 16 deg. C.

The ignition voltage has been reduced to less than 22 volts by the auxiliary current of 2.5 amps already referred to and which flows through *a* (fig. 1). Auxiliary ignition must be furnished separately for each valve in view of the single-phase design adopted. It has, however, been found possible to avoid using three auxiliary anodes in each valve (one for ignition and two for maintaining the cathode spot). A single anode *a* performs both functions since it is fed with direct current. The direct current is furnished for all phases (valves) in common from a specially-provided rectifier rated for a low voltage and low power. This auxiliary rectifier operates through a thermionic valve.

---

[4]) Actually only the single-phase design has made it possible to do away with the condensation chamber; in a six-phase valve of small volume constructed on corresponding lines to the type described here (with mercury cathode in a chrome-steel chamber) it would not have been so easy to localise the discharge within the cooled metal portion of the valve.

The voltage-drop depends on the current intensity and the temperature, and varies between 10.5 and about 18 volts, with an average of 15 volts. In the case of new valves, or where the cathode spot is not sufficiently stable, it may be slightly higher (up to 25 volts). *Fig. 3* shows the variation of the voltage-drop in relation to the load.

The back-firing voltage in the case of the valve shown in fig. 2 is about 500 volts. The valve operates with 100 per cent reliability up to 250 volts.

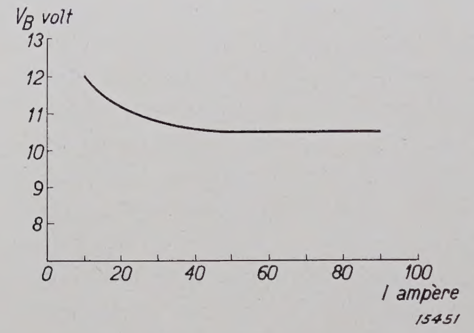

Fig. 3. The voltage-drop $V_B$ plotted as a function of the load $I$ for the new rectifying valve, measured with direct current.

The efficiency depends on the rectified power. The total losses in the valve at full load are 1150 watts, including the consumption for auxiliary ignition. The efficiency at 220 volts and 75 amps is therefore 93 per cent and at 120 volts and 75 amps 88 per cent.

Regarding the life of these valves no numerical data can yet be furnished, as up to the present not a single one of the valves (which have been under test for more than a year) has failed. The life therefore amounts in any case to many thousands of hours.

## Use of the Valve in a Rectifying Unit.

*Fig. 4* gives the circuit lay-out and *fig. 5* a photograph of a 58-kilowatt (450 amps, 130 volts) rectifying unit erected in one of the power stations of the Philips Works. The direct current circuits of the factory shops are designed for this voltage and are fed at different points from the power stations.

Hitherto rotary converters have been used for this purpose and owing to the impulsive loads (e.g. for feeding lathes, etc.) each of these had

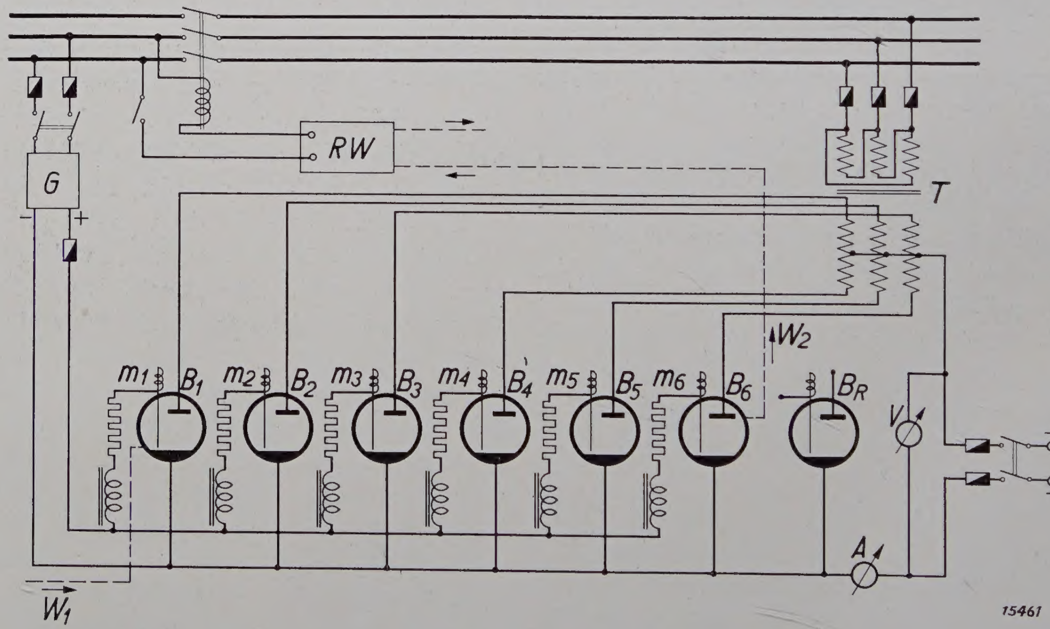

Fig. 4. Circuit connections of a rectifying unit rated for 130 volts and 450 amps. This unit is equipped with six sealed mercury-cathode metal rectifying valves $B_1$ to $B_6$. $B_R$ is a spare valve. Each valve is ignited by means of its own auxiliary anode and a magnetising coil ($m_1$ to $m_6$). The auxiliary anodes are fed from a common and independent thermionic rectifier $G$. For water cooling, the valves are divided into two groups, of three valves each. Each group has a water-actuated relay $RW$ which switches off the unit on any interruption of the water supply. (In this diagram only one water-actuated relay is shown and the water pipes are only indicated at the inlet of the first and the outlet of the sixth valve).

to be liberally rated. Thus under normal conditions they are run at loads considerably below their ratings and hence with a low efficiency. The rectifiers described here are much better suited for this purpose. Their efficiency remains satisfactory even with loads far below their ratings, and impulsive loads can be handled without inconvenience.

Brief reference must be made to some of the principal features of the rectifying unit. The water cooling systems of the six valves are divided into two groups, each of three valves connected in series, so that the water consumption of the whole unit is not greater than that required for two of the valves. A water-actuated relay *RW* has been introduced into the water supply (fig. 4) which cuts off the whole unit if the circulation is interrupted for any reason.

The auxiliary ignition is fed from a rectifier *G*, whose power consumption is the product of the D.C. voltage of 30 volts and the sum of the auxiliary currents. The auxiliary currents for all six auxiliary anodes are smoothed separately. Each auxiliary current draws its own auxiliary anode *a* out of the mercury by means of the magnetising coils $m_1$, $m_2$, etc. If the arc in any valve breaks the valve is thus re-ignited automatically.

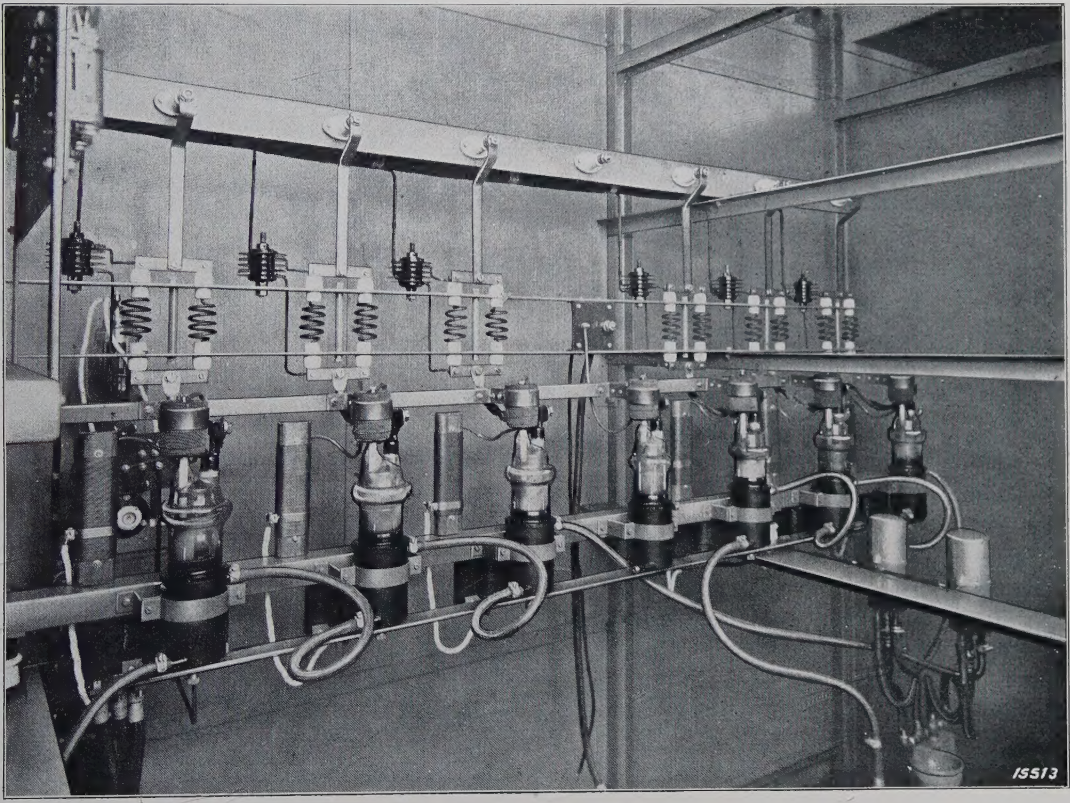

Fig. 5. Photograph of the unit shown in fig. 4. The middle valve of the seven shown is the spare valve which is not connected in the operating circuit. On the extreme righthand side the two water-actuated relays for the two cooling circuits are shown. On the left is the thermionic rectifier for the auxiliary direct current (ignition). A back-firing relay, which is not included in fig. 4, is to be seen fixed above each valve.

# COMPARISON BETWEEN DISCHARGE PHENOMENA IN SODIUM AND MERCURY VAPOUR LAMPS

## II.

**Summary.** An analysis of certain fundamental phenomena in the mechanism of discharges through gases gives important conclusions regarding the properties of sodium and mercury vapour lamps. Use is made in this article of the characteristics of excitation and ionisation of sodium and mercury discussed in a previous issue of this Review [1]). Discussion is here limited to the middle portion of a long discharge column.

### Conduction of Electricity through Gases

In its simplest form a gaseous discharge takes place in a vessel with two electrodes $C_1$ and $C_2$ (*fig. 1*) which are fused through the walls and connected to a source of current through a resistance $R$, necessary for limiting the current flowing. The current from $C_1$ to $C_2$ is conveyed by ions and electrons. The electrons travel towards the positive pole ($C_1$) where they are absorbed, while the ions travel to the negative pole ($C_2$) and combine with the electrons emitted from this electrode to form neutral atoms. Thus at both plates the carriers of the charge are destroyed, while other carriers are lost through recombination at the walls of the vessel or in the gas space.

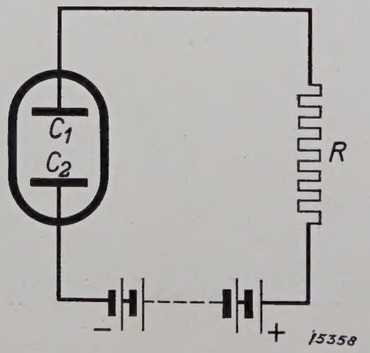

Fig. 1. Circuit diagram of a gas-discharge.

To maintain a continuous flow of electricity through gases it is necessary that under suitable conditions the gas of itself attains a state such that the generation of ions (ionisation) exactly balances the rate of recombination. If ionisation is greater than the rate of recombination, the strength of the current will increase. As a result the voltage-drop at the resistance $R$ will rise and the voltage across the poles $C_1$ and $C_2$ will drop. In response to these changes ionisation will also in general decrease and the discharge tends towards a stationary state. But the external resistance $R$ is an essential sine qua non for the attainment of this equilibrium.

In the middle portion of a long column, to which for the sake of simplicity the present discussion will be limited, the stationary state is determined by the equilibrium between the ionisation in the gas space and the recombination of ions and electrons at the walls. The emission of light, which as regards practical applications is of main interest to us, depends on other phenomena which were described in part I of this paper and which are of secondary importance in the mechanism of electrical conduction.

The obscurity in which the mechanism of gaseous discharges is shrouded is mainly due to the vast multiplicity of the types of particles present even in a simple atomic gas (i. e. a gas in which the atoms have not combined to form molecules). In addition to atoms in the fundamental state, electrons, atoms in different states of excitation and light quanta of different frequencies also occur. The state of equilibrium referred to above is determined by the mutual interaction of all these various particles.

An insight into the complex phenomena ruling is best obtained by a consideration of the limiting cases:

1. Low current-density,
   low vapour-pressure.
2. High current-density,
   high vapour-pressure.

As shown in the first part of this article already published the limiting case 1 is represented by the sodium vapour lamp, the limiting case 2 by the mercury vapour lamp. The point of view adopted here is therefore particularly suitable for an analysis of the discharge characteristics in these two types of lamp.

---

[1]) Philips techn. Rev. **1**, 2, 1936.

### Low pressure discharge. Motion of Ions and Electrons

In the column of gas discharges, electrons and ions occur with the same space-charge density, but owing to their greater mobility, the electrons carry practically the whole of the current. The energy imparted to them per cub.cm, viz: Energy per $\mathrm{cm}^3$ = Current density × longitudinal field-strength (gradient) is transmitted by various processes to the atoms in the gas or to the walls of the containing vessel and is finally radiated in the form of light and heat.

The smallness of the kinetic energy transmitted from the electrons to the atoms, which is related to the large difference in the masses $m$ and $M$ of the electrons and atoms respectively has a very important bearing on the motion of the electrons. The maximum energy $E$ imparted to an atom at rest by a single elastic collision is:

$$E = \frac{4m}{M}\,\varepsilon \quad . \; . \; . \; . \; . \quad (1)$$

where $\varepsilon$ is the energy of the electron. According to equation (1) at most 1/10,000th part of the energy of the electron is given up on a single elastic collision in the case of sodium vapour, and at most 1/100,000th part in the case of mercury vapour. On the other hand by ionisation or excitation, the electron can impart its whole kinetic energy to an atom. Appreciable transmission of energy to the gas atoms therefore is only initiated when the electrons have derived sufficient energy from the electric field to produce atomic excitation. A state is therefore established in which the mean kinetic energy of the electrons is comparable with the energy of excitation, whilst the mean energy of the atoms does not assume a greater value than that corresponding to the temperature of the vapour. The temperature of the sodium vapour at the wall of the tube is approximately 280° C. In the axis of the discharge column the temperature is about 50 degree higher. The mean kinetic energy of the free electrons is of the order of 2 electron-volts ²). Such a high mean energy would only be acquired by the atoms at a temperature of 15000 °K. This fact is sometimes stated by saying that the „temperature of electrons" is 15000 °K. *Table I* gives electron temperatures such as are met with in sodium lamps at different vapour pressures.

Equation (1) is derived from the equations of energy and momentum. The maximum energy is transmitted from an electron to an atom on central collision (*fig. 2*). Denoting the velocity of atom and electron before collision as $V$ and $v$ and after collision as $V'$ and $v'$ respectively and assuming the atom to be at rest before the impact ($V = 0$) the following equations are obtained:

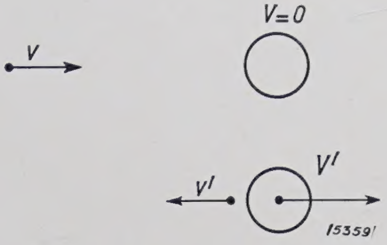

Fig. 2.

Conservation of energy:

$$\frac{m}{2}\,v^2 = \frac{m}{2}\,v'^2 + \frac{M}{2}\,V'^2$$

Conservation of momentum:

$$mv = mv' + MV'$$

Eliminating $v'$ one obtains:

$$V' = \frac{2\,m\,v}{M+m}$$

which on substituting the kinetic energies:

$$E = \frac{M}{2}\,V'^2$$

$$\varepsilon = \frac{m}{2}\,v^2$$

leads to the result:

$$E = \frac{4\,mM}{(M+m)^2}\,\varepsilon$$

or approximately

$$E = \frac{4m}{M}\,\varepsilon$$

The assumption that the atoms are at rest before collision is justified by the very marked difference in the mean kinetic energies of atoms and electrons. Owing to their higher velocity more electrons than ions impinge on the wall of the discharge tube, which thus become negatively charged. As a result subsequent electrons are repelled and ions attracted, so that the ionic current at the wall becomes just as great as the electronic current. The wall, however, always remains negatively charged. The path described by the ions is shown diagrammatically in *fig. 3*. It is seen that ions which are produced in the discharge soon terminate at the walls after traversing a short path. There they recombine with electrons of the wall charge to form neutral atoms and give up the ionisation energy liberated to the walls in the form of heat.

---

²) The unit electron-volt ($eV$) is the energy which an electron must expend in order to overcome a voltage drop of 1 volt. 1 $eV$ = 1.59 $10^{-19}$ watt-sec.

## Excitation and Ionisation Processes dependent on Pressure and Current Density

In very rarefied gases and with small current-densities the frequency of excitation and ionisation reactions is proportional to the product of the concentrations of electrons and atoms in the fundamental state. The number of excited atoms is then relatively small and has no influence on the reactions taking place. The probability of excitation is closely governed by the velocities of the free electrons and by the properties of the individual atoms. In general excitation of the resonance state is particularly favoured. Thus, **Krefft, Reger** and **Rompe**[3]) found that in sodium vapour at a pressure of 0.005 mm and a current density of 0.05 A per sq.cm 95 percent of the energy of the electrons is utilised for excitation and emission of resonance light.

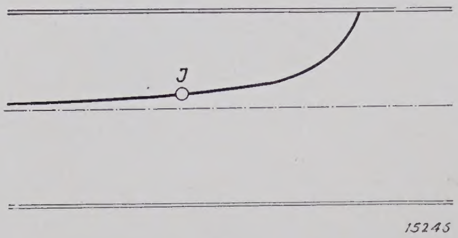

Fig. 3. Path of the ions $J$ in a discharge through gases.

In the sodium lamp somewhat higher pressures and current densities are in general used than in the experiments of **Krefft, Reger** and **Rompe**, whereby owing to the intervention of secondary processes, the excitation processes become extraordinarily complex.

However, in a qualitative sense, it can be readily conceived that the intensity of the resonance light will become diminished as compared with the intensity of the higher transitions and that the concentration of the ions will increase to a greater degree than the concentration of the excited atoms. Responsible for this transformation are self-absorption, collisions of the second kind and cumulative excitation.

## Self-absorption and Secondary Processes

Light quanta of the resonance line become absorbed, after traversing a short path $S$, by an atom in the fundamental state, resulting in the latter's excitation to the resonance state, and are re-emitted in no particular direction by the excited atom. These quanta thus describe a very long wandering path if the density of the gas is not too small, which with a tube of radius $R$ is made up of

$$Z = (R/S)^2$$

absorptions and re-emissions before a particular quantum of light escapes from the tube. As the number of absorptions $Z$ increases, there is a greater probability that one of the atoms will be excited from the resonance state to a higher energy level by electron impact (cumulative excitation) or inversely transfer its energy to the colliding electron thus returning to the fundamental state without emission (collision of the second kind). Both these processes produce a weakening of the resonance radiation. The calculation of $Z$ is rendered very difficult by the heterogeneity of the radiation, which latter does not possess a single well-defined wave-length, but an intensity distribution covering some hundredths of an Ångström unit and giving a spectral line of finite width. The wings are subject to much less absorption than the core. The calculation of the free path $S$ thus stipulates a knowledge of the shape of the spectral line, which in turn undergoes marked alteration owing to self-absorption. (See *fig. 4*). These processes have been investigated theoretically by **de Groot**[4]) and **Kenty**[5]). Under average operating conditions, the value of $Z$ for sodium lamps is estimated to be of the order of 1000 to 10000. Self-absorption reduces the concentration of the atoms in the fundamental state and intensifies excitation to higher levels including the ionized state. At a given velocity distribution for the electrons, the secon-

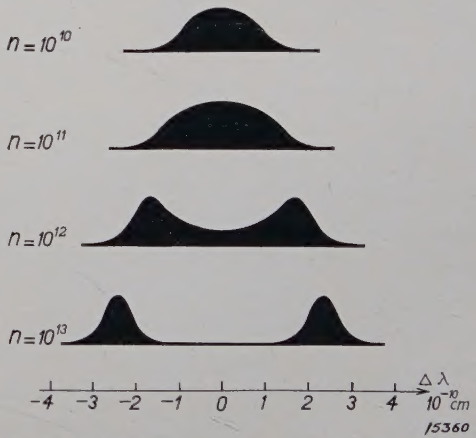

Fig. 4. Spectral distribution of resonance radiation at various concentrations of the sodium vapour. The curves are calculated for a layer thickness of 2 cm. $n$ is the number of atoms per cub. cm. (Reproduced from W. **de Groot**, Physica **12**, 289, 1932).

---

[3]) H. **Krefft**, M. **Reger** en R. **Rompe**, Z. f. techn. Phys. **14**, 242, 1933. M. J. **Druyvesteyn**, Phys. Z. **33**, 822, 1932.

[4]) W. **de Groot**, Physica **12**, 289, 1932; **13**, 41, 1933.

[5]) Carl **Kenty**, Phys. Rev. **40**, 633, 1932; **41**, 390, 1932; **42**, 823, 1932.

dary processes thus produce an augmentation of ionization greater than in proportion to the concentration of the electrons and the atoms. This has an important bearing on the interpretation of the characteristics of discharges in gas tubes.

### Effect of Pressure and Current Density on the Voltage Gradient

At a constant pressure the recombination of ions and electrons occurring at the walls is proportional to the current density. As no excess of ions can be produced, the same also applies to ionisation. With a constant velocity distribution of the electrons, however, as shown in the preceeding chapter, ionisation would increase more than the relative increase in current density. Hence, in view of the stability of the discharge referred to at the outset, it may be expected that as a result of a drop in the voltage gradient the velocities of the electrons will diminish and the ionisation will be restored to the correct measure. The decrease of the gradient with rising current density is known as the negative resistance of the discharge. For stability to be obtained it is necessary for the external resistance to be sufficiently great to make the total resistance positive. Also if the current strength is constant and the pressure increased, the mean kinetic energy of electrons will fall and thus compensate the increasing influence of cumulative processes. *Table I* gives details of measurements taken of sodium tubes by Druyvesteyn and Warmoltz[6]) which confirm this interpretation.

**Table I**

| Vapour pressure | Current | Gradient | Energy of electrons | |
|---|---|---|---|---|
| mm | Ampere | Volt per cm | Volt | Temp. °K |
| $2 \cdot 10^{-3}$ | 0.2 | 0.432 | 4.00 | 30900 |
| | 1.0 | 0.398 | 2.48 | 19200 |
| $8 \cdot 10^{-3}$ | 0.2 | 1.082 | 3.80 | 29400 |
| | 1.0 | 0.668 | 1.24 | 9600 |

The table gives data of the voltage gradients and the temperature of the electrons at two vapour pressures ($2 \cdot 10^{-3}$ mm and $8 \cdot 10^{-3}$ mm), which correspond to wall temperatures of 255 and 287 deg. C. On increasing the current from 0.2 A to 1 A, the voltage gradient and the energy of the electrons decrease for both vapour pressures. Furthermore, the energy of the electrons also decreases at constant current density and increase in the vapour pressure, so that the "electron temperature" $T_e$ and the temperature of the vapour $T_g$ converge.

### Transition to the high-pressure Discharge

The variation in the electron temperature at constant current density and rising vapour pressures has been studied over a wider range with discharges through mercury vapour than with discharges through sodium vapour. With mercury vapour also, $T_e$ and $T_g$ approach each other as the pressure rises. As shown in *fig.* 5, these two temperatures are practically equal at pressures above 30 mm. At these vapour pressures a thermal equilibrium between the electrons and atoms has been attained. The thermal equilibrium is a characteristic feature of the high-pressure discharge.

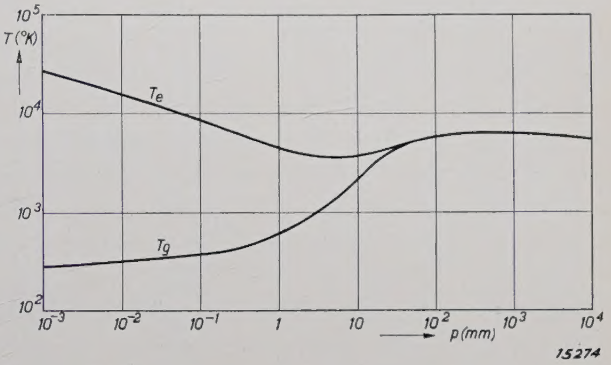

Fig. 5. Electron temperature $T_e$ and vapour temperature $T_g$ at constant current strength and different vapour pressures. (Diagrammatic.) Reproduced from W. Elenbaas, Ingenieur **50,** E 83, 1935.

### High-pressure Discharge

Whilst the transition processes between the limiting cases are very complex, the high-pressure discharge itself can be described more easily.

At thermal equilibrium the degrees of excitation and ionisation can be deduced from statistical considerations without any knowledge of the atomic mechanism. For the density $n_a$ (per cub.cm) of the excited atoms, the Boltzmann equation applies:

$$n_a / n_o = e^{-\frac{\varepsilon_a}{kT}} \quad . \quad . \quad . \quad . \quad . \quad (2)$$

where $n_0$ is the density of the atoms in the fundamental state $\varepsilon_a$ the excitation energy, $k$ the molecular gas constant of Boltzmann[7]).

---

[6]) M. J. Druyvesteyn and N. Warmoltz, Phys. Z. **33,** 822, 1932; Phil. Mag. **17,** 1, 1934.

[7]) The molecular gas constant $k$ is related to the molar gas constant $R$ by the formula: $R = k \cdot N$ where $N$ is the number of molecules per gram-molecule. ($N = 6.06 \; 10^{23}$, $k = 1.37 \; 10^{-16}$ erg per degree.)

The density of excited atoms determines the intensity of radiation in the corresponding wavelengths.

Ionisation may be regarded as dissociation of the gaseous atoms into ions and electrons. The degree of ionisation $a$ can be calculated from the equilibrium condition between ions and electrons and neutral atoms by means of the law of mass action. The dissociation equilibria are thus given by the equation:

$$\frac{a^2 n_o}{1-a} = C\ (T) \quad . \; . \; . \; . \quad (3)$$

where $C$ is a function of the temperature containing the energy $\varepsilon$ of ionisation in the Boltzmann factor $exp\ (-\ \varepsilon_i/kT)$. Saha 8), calculating the value of the constant $C$ for ionisation equilibria in ideal gases, found:

$$C = \frac{(8\ \pi\ m\ kT)}{2\ h^3}^{3/2} e^{-\frac{\varepsilon_i}{kT}}$$

whereby $h = 6.55 \cdot 10^{-27}$ ergsec (Cf. Nr. 1, p. 3 of this journal). Introducing the concentration $n_i$ of excited atoms: $n_i = a\ n_o$, one computes from equation (3) with the numerical values of $m$, $k$ and $h$:

$$\frac{n_i^{\ 2}}{n_o - n_i} = 0{,}98 \cdot 10^{-16}\, T^{3/2}\, e^{-\frac{\varepsilon_i}{kT}}\ \mathrm{cm}^{-3}\ . \quad (4)$$

This expression determines the concentration of ions as a function of the temperature.

## Mechanism of Discharge at Thermal Equilibrium.

At thermal equilibrium the conditions of discharge are completely described by the temperature $T$ in the cylindrical discharge tube as a function of the radius $r$. Knowing the temperature distribution, one can compute as a function of the radius:

1) The concentration $n_i$ of thermal ionised atoms and thus the current density, given by

$$j = n_i\ (\beta_i + \beta_e)\ G$$

where $G$ means the gradient, $\beta_i$ and $\beta_e$ the mobilities of ions and electrons.

2) The concentration $n_a$ of thermal excited atoms and thus the intensity of radiation in the different wavelengths.

3) The power $j \cdot G$, supplied per cub.cm and thus, after subtraction of the radiation power, the heat development $Q$ per cub.cm and sec.

The temperature distribution is given by the laws of thermal conduction. The heat flow is proportional to the temperature-gradient and for a cylindrical surface of radius $r$ is:

$$q = 2\pi\ r\ \frac{dT}{d\,r}\ \sigma \quad . \; . \; . \; . \; . \; . \; . \quad (5)$$

where $\sigma$ means the coefficient of thermal conduction and is a function of the temperature. From equation (5) it is simple to derive a differential equation for the temperature distribution. Consider a cylindrical volume element with a thickness $dr$. The difference $dq$ between the heat influx and heat efflux is equal to the amount of heat generated in the element of volume per second. This is $2\ \pi\ r\ dr.\ Q\ (r)$, where $Q(r)$ is the amount of heat developed per cub. cm per sec. Thus:

$$\frac{dq}{dr} = 2\ \pi\ r\ Q(r)$$

or substituting for $q$ from equation (5):

$$\frac{d}{dr}\left[\ 2\ \pi\ r\ \frac{dT}{dr}\ \sigma\right] = 2\ \pi\ r\ Q(r) \quad \ldots\ldots \quad (6)$$

As shown above, the heat development $Q$ can be calculated as a function of the temperature. Substituting this function in equation (6), one obtains a differential equation for the temperature which contains no arbitrary coefficient. This equation was analysed by Elenbaas 9) for discharges through high-pressure mercury vapour and for a particular case (vapour pressure $P$ = 1 atmos., power input $N$ = 40 watts per cm of the discharge column) gives the temperature distribution shown in *fig. 6*. The temperature at the middle of the discharge path is above 6000 deg.

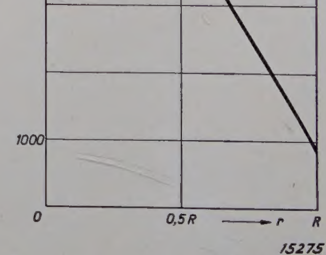

Fig. 6. Temperature in a mercury vapour discharge (in deg. abs.) as a function of the distance $r$ from the axis of the discharge tube. Vapour pressure 1 atmos., power input 40 watts per cm, diameter of tube 2cm. Reproduced from W. Elenbaas, Ingenieur **50**, E83, 1935.

---

8) M. N. Saha, Phil. Mag. **40**, 472, 1920; Z. f. Phys. **6**, 40, 1921.

9) W. Elenbaas, Physica **1**, 673, 1934.

abs. Concordance between the calculated current density and the measured values was satisfactory. The differential equation can, however, not be strictly correct as the transfer of energy by radiation as compared with thermal conduction has been neglected.

### Contraction of the Column

The constriction of the path of the discharge is the visible indication of the transition from the mechanism of electronic collision to the thermal form of discharge. This phenomenon is readily explained from the temperature distribution shown in fig. 5. At the hottest part, i.e. along the centre, ionisation and hence the current density has the greatest value. *Fig.* 7 shows as a function of the radius:

a) The current density (theoretical)

b) The intensity of the yellow mercury lines (experimental measurement).

Curves a) and b) show qualitatively the same trend, but curve b) is wider. This is chiefly due to the fact that in the external zones of the discharge where, in consequence of the lower temperature, practically no more ionisation takes place, there is still a slight emission of light, owing to absorption and re-emission of light quanta emanating from the hot internal zone. This phenomenon is treated more in detail in part I of the article. (See this periodical, page 4, Januari 1936).

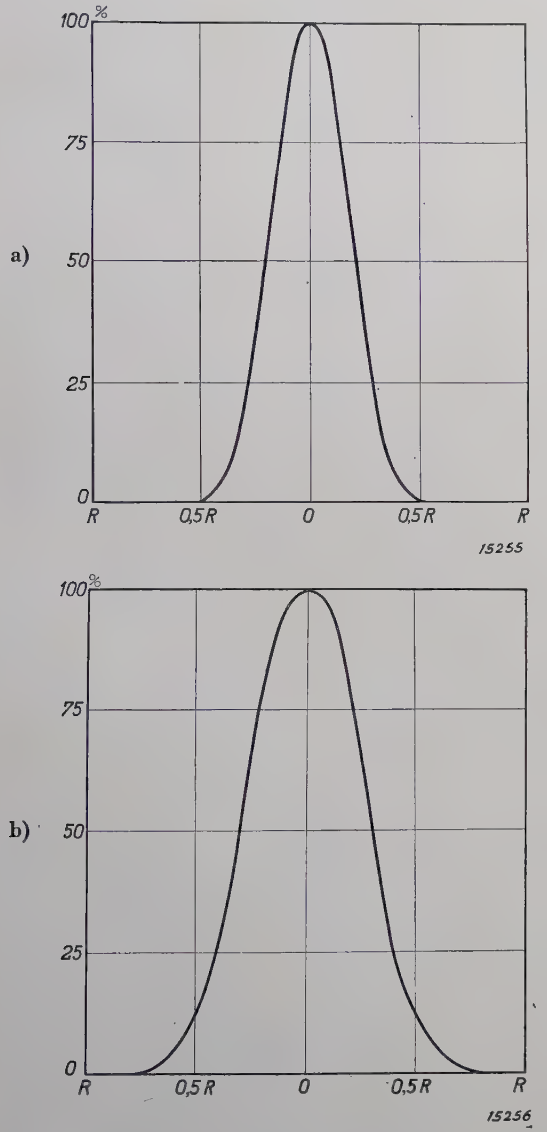

Fig. 7. a) Calculated current strength.
b) Measured intensity of the yellow lines at 5770/90 Å as a function of the distance $r$ from the axis of the tube for a mercury-vapour discharge at a pressure $P = 1$ atmos and a power $N = 40$ Watt per cm. (Relative units).

### Conclusions to Parts I and II

The visible light of the sodium lamp chiefly comes from resonance radiation. Radiation corresponding to higher transitions is generally infra-red. On the other hand the visible light from the mercury vapour lamp is due to transitions between higher levels; the resonance lines are ultra-violet.

Resonance light is principally radiated at low current densities and gas pressures. Excitation then takes place owing to electron impact upon atoms being in the fundamental state. Transitions between higher excited levels are favoured at high current strengths and pressures. Resonance light is then weakened by self-absorption and collisions of the second kind; the excitation of higher states is promoted by cumulative processes.

By such considerations one is led to run sodium lamps from which a marked resonance radiation is desirable with the lowest possible current densities and pressures. A limit is here set by the fact that the heat evolved must give a sufficiently high operating temperature (280 deg. C) with suitable types of insulation. On the other hand, mercury vapour lamps give the highest efficiency at very high current strengths and pressures, and are therefore designed in the form of high-pressure discharges. The limits are here set by the pressures and temperatures which can be maintained technically.

At the practical limits sodium vapour and mercury vapour radiate their characteristic luminous rays with approximately the same efficiency.

Compiled by G. HELLER.

# DEMONSTRATION MODEL ILLUSTRATING SUPERHETERODYNE RECEPTION

### Introduction

At the World Exhibition held in Brussels last year, a demonstration model was exhibited which illustrated in the most elementary manner the method of operation of modern radio receivers. It is of course generally known that in radio transmission a carrier wave of high frequency is employed and the much lower audio-frequencies are transmitted as a modulation of the amplitude of this carrier wave. The function of the rectifying stage in the receiver is to separate these low audio-frequencies from the high frequency of the carrier wave. Perhaps less well known is the sequence of operations which actually take place in a superheterodyne receiver in which an "oscillator", a "converter valve" and an "intermediate frequency" are used. The main object of the demonstration model described in the present article is therefore to illustrate the principles underlying superheterodyne reception.

### The Superheterodyne Principle

In superheterodyne receivers, not only is the incoming high-frequency carrier wave appropriately dealt with, but provision is also made for the simultaneous generation of an additional oscillation by means of an oscillator, the frequency of this local oscillation differing by a specific number of cycles per second from the frequency of the carrier wave. The function of the converter valve is to reduce modulation to a new carrier wave of lower frequency. This is done by producing a periodic fluctuation in the amplification of the incoming wave in synchronism with the self-generated auxiliary oscillation of the oscillator. The alternating current $I_a$ in the anode circuit of the converter valve is given by the product of the gradient $S$ of its characteristic and the amplitude $V_g$ of the alternating current component of the grid potential, thus:

$$I_a = S\, V_g \quad \ldots\ldots\ldots\ldots\ldots\ldots\ldots (1)$$

The gradient $S$ is now varied with the angular frequency $\omega_h$ of the auxiliary oscillation, while the grid potential $V_g$ varies with the angular frequency $\omega_i$ of the incoming carrier wave. For the sake of convenience we shall express the conditions obtaining simply as sine functions:

$$S = S_o + a \cos\omega_h t \quad \ldots\ldots\ldots (2)$$

$$V_g = \beta \cos\omega_i t \quad \ldots\ldots\ldots\ldots (3)$$

In the expression for the anode current $I_a$ we then have the term:

$$a\, \beta \cos\omega_h t \cos\omega_i t$$

which can be resolved into two terms containing the sum and the difference respectively of the frequency of the carrier wave and of the auxiliary oscillation, thus:

$$I_a = \ldots. + \frac{a\beta}{2} \left\{ \cos\left(\omega_h + \omega_i\right) t + \cos\left(\omega_h - \omega_i\right) t \right\} \ldots (4)$$

The differential frequency $(\omega_h - \omega_i)$, which is also termed the intermediate frequency, is then filtered out in the receiver. The differential-frequency circuits are very accurately tuned to an intermediate frequency-band at 125 kilo-cycles, which from now on acts in the receiver as the new carrier wave of the audio-frequency modulation. For if $\beta$ in equation (3) is not constant, but varies with the audio-frequencies to be transmitted, then according to equation (4) the amplitude of $I_a$ also will fluctuate with the same frequency. After suitable amplification, the intermediate-frequency carrier wave is separated in the usual way in the rectifying section of the receiver from the low-frequency modulation, which it is required to render audible in the loudspeaker.

The chief advantage of superheterodyne reception as compared with direct amplification and elimination of the high-frequency carrier wave is that the tuning of the intermediate-frequency circuits by the reception of stations operating with very different high-frequency carrier waves can always be very accurately maintained at the individual intermediate-frequency bands. Particularly the desire to make receiving apparatus capable of receiving, in addition to ordinary radio waves, also very short wave lengths, has been responsible for the adoption of the superheterodyne principle in radio reception.

### The Octode

To generate the auxiliary oscillation and to modulate it on the incoming oscillation a special converter valve, the octode, is used in Philips superheterodyne receivers. This valve may be regarded as a triode and a pentode, connected in series, in which the triode serves for the generation of the auxiliary oscillation, while the pentode further handles the alternating current generated in the triode.

In the diagrammatic sketch in *fig. 1* the grids are marked from *1* to *6*. The indirectly-heated cathode together with the control grid *1* and the auxiliary anode *2* constitute the triode. The control grid *1* is connected to the oscillating circuit $L_1C_1$ which is tuned to the auxiliary frequency. $L_2$ is a reaction coil connected to the auxiliary anode *2*, while a third grid serves for screening the triode against the pentode. In the latter, *4* is the control grid, *5* the screen-grid and *6* the interceptor grid connected to the cathode, which prevents the secondary electrons emitted from the various grids and the anode from contributing to the anode current. The control grid *4* is in circuit with the tuned aerial circuit $L_3C_3$.

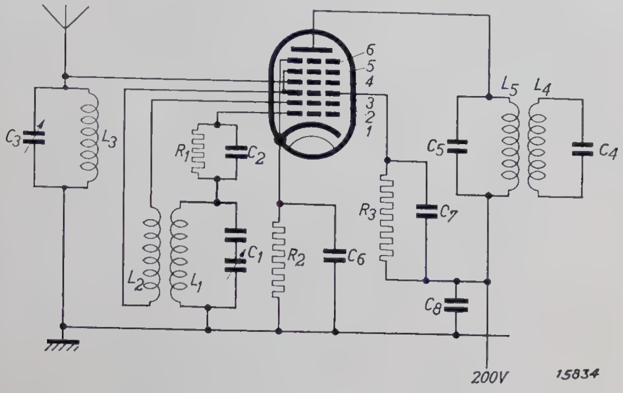

Fig. 1. Circuit diagram of the octode. The circuit $L_1C_1$ is tuned to the auxiliary oscillation, $L_3C_3$ to the incoming signals, $L_5C_5$ and $L_4C_4$ to the intermediate frequency.

*1* = Control grid
*2* = Auxiliary anode
*3* = Screen-grid
*4* = Control grid
*5* = Screen-grid
*6* = Intercepter grid

The potential applied to grid *1* varies in synchronism with the auxiliary frequency. As a result the electrons emitted from the cathode can only intermittently pass through the control grid *1*. An electron stream is therefore obtained in the pentode whose intensity varies with the auxiliary frequency. The amplification factor in the pentode of the converter valve will thus also vary periodically with the auxiliary frequency according to equation (2). The incoming oscillation, which has to be amplified, is applied to the control grid *4* of the pentode. This grid will therefore allow a more or less free passage to the electron stream in synchronism with the frequency of the incoming carrier wave, since its potential varies according to equation (3). In the anode circuit, resultant currents will therefore be obtained with either the additive or differential frequency of the auxiliary oscillation and the carrier wave, as expressed by equation (4). The connected circuits of the receiver, $L_5C_5$ and $L_4C_4$, are accurately tuned to the differential frequency, which is filtered out here and then passed to the rectifying stage as described above.

## Mechanical representation with the aid of sand figures

Electrical oscillations are usually represented diagrammatically by means of a sinusoidal or similar type of wavy line. It appeared therefore that these oscillations, which are usually drawn with chalk on a blackboard, could be usefully reproduced mechanically for general exhibition by means of a sand figure on a slowly-moving belt. This would enable a practical demonstration of the principles of reception and the properties and uses of the carrier wave. In the demonstration model which was evolved for this purpose, the utilisation of the actual carrier wave is also demonstrated by means of a number of cathode ray tubes, which produce a visible trace of the electrical oscillations on their fluorescent screens.

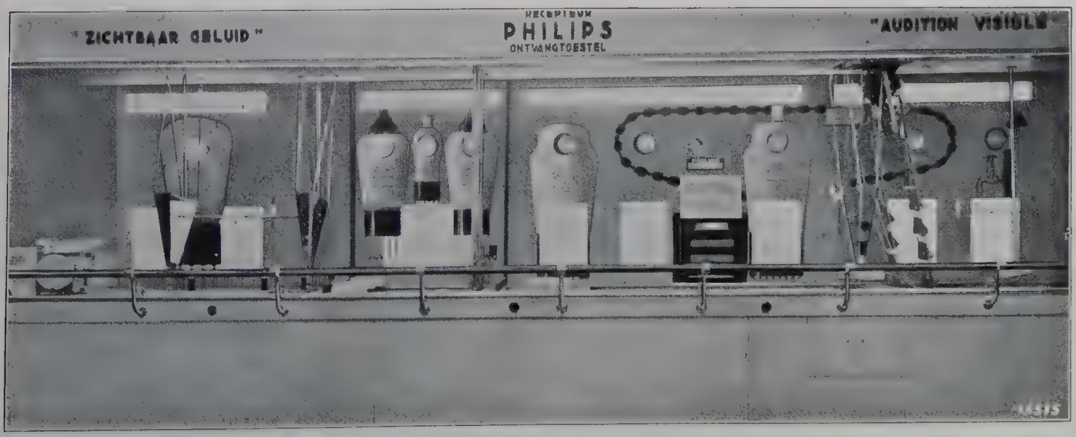

Fig. 2. Front view of model demonstrating superheterodyne reception, as shown at the Brussels 1935 World Exhibition.

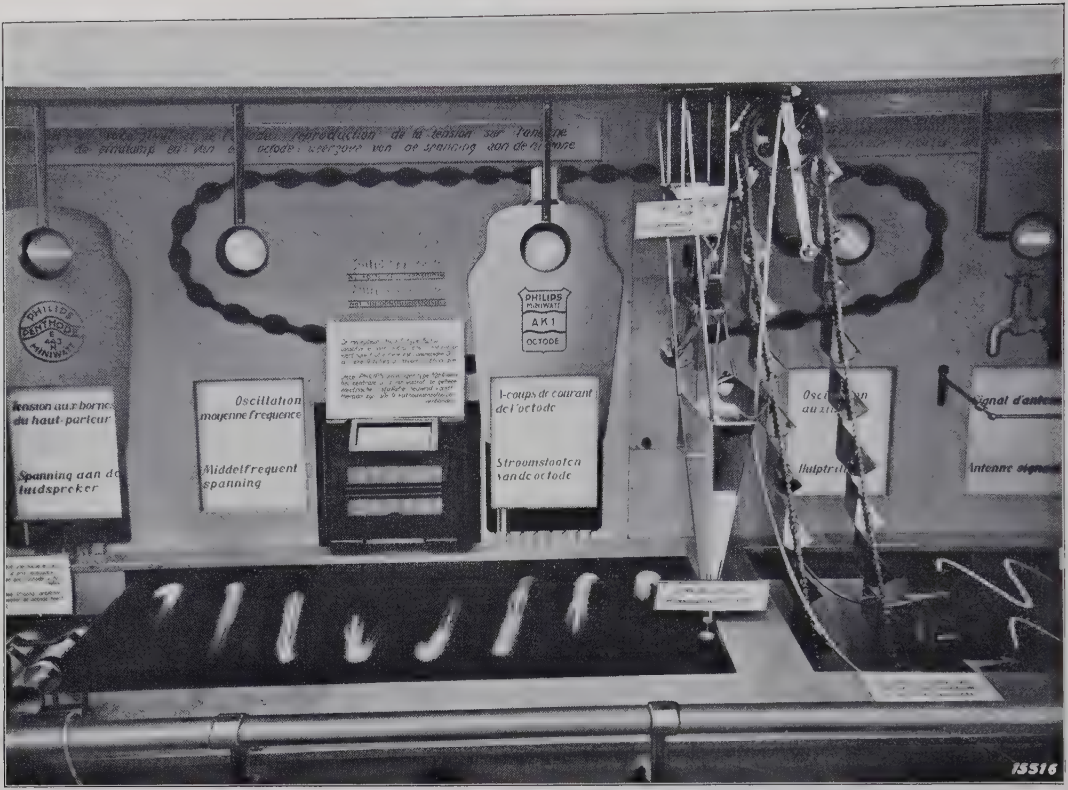

PHILIPS PENTHODE E 443 N MINIWATT
Tension aux bornes du haut-parleur
Spanning aan de luidspreker
Oscillation moyenne frequence
Middelfrequent spanning
PHILIPS MINIWATT AK1 OCTODE
I-coups de courant de l'octode
Stroomstooten van de octode
Hulptril
Antenne signaal
15516

Fig. 3. Sand figures demonstrating the anode current of the octode.

In *fig. 2* the apparatus is shown which was exhibited on the Philips stand at Brussels. The graphing of the various oscillations occurring in radio receivers in the form of sand figures is performed on a moving belt which moves in a horizontal direction from right to left. The belt is only just visible in this picture, but is more clearly shown in *fig. 3*. The feed tubes for the sand and the pendulums fitted with funnels which swing to and fro from back to front and thus produce the sand figures, can be picked out in fig. 1. *Fig. 4* is a diagrammatic sketch of the arrangement. The conveyer belts running from right to left are shown dotted in fig. 4b (*I*, *II*, ...). Above them are the funnel-shaped and tubular sand distributors (*1*, *2*, ...). Fig. 4a depicts the sand figures as they are produced on the horizontal moving belts.

The carrier waves of the incoming oscillations is shown in fig. 4a by curve *A*; the sand distributor *1* swings to and fro, while at the same time the belt *I* moves from right to left so that a sinusoidal or wavy line is traced. The modulation of the carrier wave has not been taken into consideration here as even with a very high musical note of for instance 5000 cycles, modulated on a 200-metre (1500-kilocycle) carrier wave, no less than 300 carrier-wave periods are required to reproduce a single modulation period. The variation in amplitude after only a few periods would therefore be too small on the belt to be distinctly visible. The curve *B* depicts the local oscillation which is generated by the octode in the receiver. It is traced on the belt by funnel *2*.

The superposition of the carrier wave and the local oscillation is represented by means of the sand figures in the following way. The two sand figures *A* and *B* drop into a mixing box at the end of the moving belt *I* and are then transferred to funnel *3* by means of an elevator, this funnel then tracing the striking figures *C* on the second belt. These figures symbolise the current in the anode circuit of the octode. The *C* figures are traced in the following manner:

Pendulum *3* always swings in phase with pendulum *1* which traces curve *A* (incoming carrier wave), but its flow of sand is not continuous, being regulated by means of a flap which opens and closes in phase with the motion of pendulum *2*. This intermittent release of sand gives a trace of the electron stream in the triode in phase with the auxiliary oscillation. The magnitude of the anode current varies in synchronism with the incoming carrier wave, which in the demonstration model is simulated by phase equality in the motions of pendulum *3*. If the ends of the sand figures *C* are visualised as connected by an envelope, a curve is obtained which slowly fluctuates up and down

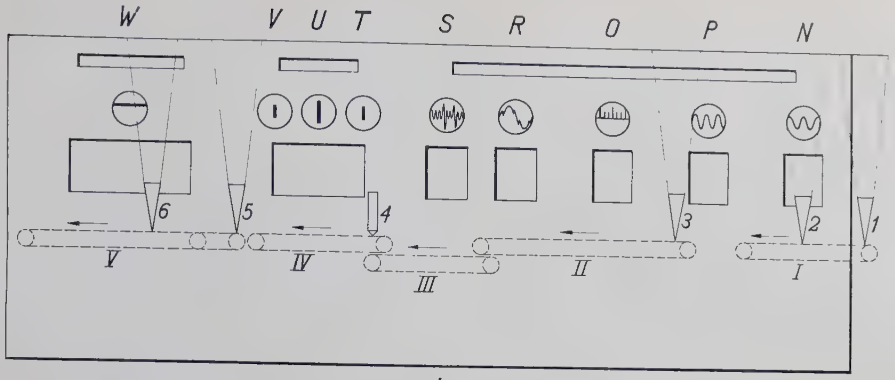

b

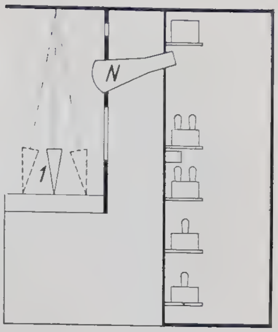

c

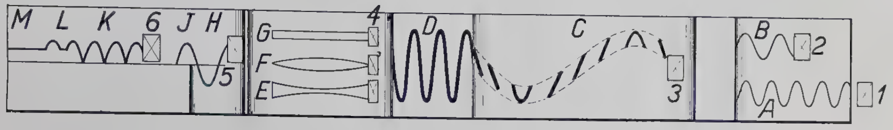

a

Fig. 4a. The belts moving from right to left on which the sand figures are traced.

*A* = Incoming signal
*B* = Auxiliary oscillation
*C* = Anode current of the octode
*D* = Intermediate-frequency oscillation
*E* = Variable magnitude of incoming signals
*F* = Amplification
*G* = Loudspeaker current, practically constant

*E*, *F*, *G* represent the automatic volume control.
*H*, *J*, *K*, *L* and *M* represent the methode of operation of the mains-fedd component of the receiver.

Fig. 4b. Diagrammatic front view of the demonstration model. *I* to *V* are the belts moving from right to left, on which the pendulums *1* to *6* trace the sand figures. *N* to *W* are the fluorescent screens of the cathode ray oscillographs on which the following voltages and currents are depicted.

*N* = Incoming signals from the aerial.
*P* = Auxiliary oscillation generated by the octode.
*O* = Variation of the anode current of the octode.
*R* = Voltage at the intermediate-frequency transformer.
*S* = Low-frequency voltage at the loudspeaker poles.
*T* = Portion of the signal voltage in first circuit of the receiver.
*U* = Amplication factor to which the receiver is automatically controlled.
V = Portion of the voltage at the loudspeaker terminals.
W = Variation of the rectified voltage.

Fig. 4c. Side view of model.

and represents the oscillation of the intermediate frequency. This behaviour can be observed in fig. 3.

In the intermediate-frequency circuits, the intermediate-frequency oscillation is filtered out from the current impulses leaving the converter valve. It then acts as a new carrier wave for audio-frequency modulation, which is what is required as it constitutes the sound emitted from the loudspeaker. As in this representation by means of sand figures modulation of the high-frequency carrier wave (pendulum *1*) has not been taken into account the converter valve of the demonstration model furnishes only an unmodulated intermediate frequency for the carrier wave. In view of the absence of modulation, rectification of the radio signals also has not been considered in the present model.

In the demonstration model, the sand figures on reaching the end of belt *II* are allowed to slide down a short inclined plane, which causes a more uniform distribution of the sand particles before the lower moving belt *III* is reached. This belt moves at a slower speed so that the sand particles falling on it produce a closed wavy curve *D* with a shorter wave-length (see fig. 4a). This curve represents the filtered oscillation of intermediate frequency as a function of a slower time parameter; thus for the sake of clearness the time axis of the sine curves, which are of principal interest here, has been slightly compressed on belt *III*.

## Representation of other factors in reception

The radio receiver also incorporates a self-regulating fading eliminator or automatic volume control whose operation is based on the following principle. The fluctuation in the unidirectional voltage, which occurs on a variation in the amplitude of the intermediate-frequency carrier wave behind the rectifying stage, is led back to the preceding valves, whereby these valves receive a greater or smaller negative grid bias. As the incoming signals fade this bias is reduced and the amplification is increased. The method of volume control is represented by the sand figures *E*, *F* and *G* (fig. 4a). *E* represents the variable intensity of the incoming carrier wave, *F* the amplification which is maintained automatically in the receiver, and *G* the voltage fed to the loudspeaker and which is practi-

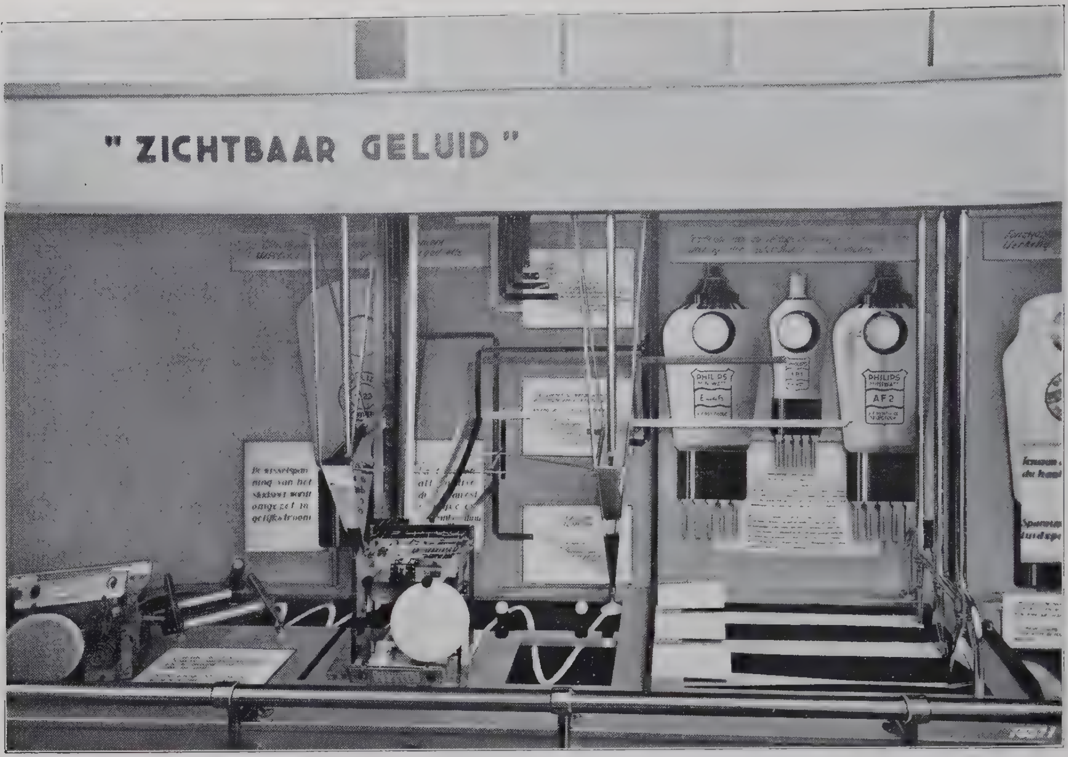

Fig. 5. Representation of automatic volume control and rectification of mains supply.

cally unaffected by the fading effect. These sand figures are traced by means of three funnels with flattened extremities from which the sand runs out (see the right half of *fig.* 5). The first two funnels can be turned about their longitudinal axis, but are coupled together in such a way that their relative positions differ by a fixed angle of 90 °. If the first funnel traces a very thin line (corresponding to a very weak incoming signal) the second funnel traces a line of maximum breadth (corresponding to maximum amplification). The third funnel traces a curve of practically constant breadth. Only when the line traced by the first funnel becomes very thin (very extreme fading) is the third funnel turned a little, so that its trace also becomes somewhat narrower.

Finally, on the last belt (*V* in fig. 4b) the operation of the two-way rectifier is represented, which furnishes the anode voltage required for the receiving valves. A pendulum *5* traces sine curves which represent the transformer voltage, where *H* is one half and *J* the other half of the wave. The rectifying valve allows current to flow through it in one direction only. An arrangement has therefore been employed here which dispenses with *H* and retains only *J*. Two-way rectification may be regarded as the combination of two separate rectifiers which operate alternately, so that each of the half-waves is rectified. To represent this a second pendulum *6* is allowed to trace a sine curve in phase opposition to the first pendulum funnel, and which traces the voltage of the other half of the transformer. After two-way rectification a pulsating rectified current is produced which is represented in sand figure *K*. The first condenser of the smoothing circuit reduces the non-uniformity of the rectified current. This is simulated in the sand figures by means of a small revolving brush which sweeps the sand towards the middle, so that figure *L* is produced. Further smoothing makes the current completely uniform and steady; thus a second brush removes the slight remaining waviness and traces figure *M* (see on the left of fig. 5).

The sand dropping off the ends of the belt is collected and is returned to the storage box by means of an elevator which is not visible to the public; at the same time it is dried to prevent the sand particles adhering to the belts.

### Demonstration with Cathode Ray Tubes

In addition to this highly slowed down representation of the processus occurring in the superheterodyne receiver, the various electrical phenomena have also been rendered visible by a series of nine cathode ray tubes whose fluorescent screens are shown in fig. 2. The alternating voltages at nine different points of the receiver are magnified by amplifiers to such values that their fluctuation can be demonstrated with the aid of the cathode ray tubes. Each amplifier has its own rectifier so that no disturbing coupling actions can be produced.

The amplified voltages are applied to the deflection plates of the cathode ray oscillographs which deflect the electron beam in a vertical direction. By means of a horizontal time-base deflection [1]) of suitable frequency the alternating current figures are traced on the fluorescent screens. The period of the time-base can be adjusted as required, but it must be a whole multiple of the alternating voltage represented.

In fig. 4b the screens of the tubes are indicated by the letters $N$ to $W$. The suffixes indicate the nature of the trace on each screen. By applying more or less quickly varying saw-tooth voltages, sinusoidal figures were obtained on the screen which showed more or fewer oscillations as indicated in fig. 4.

In place of the saw-tooth voltage variation of the time-base a sinusoidal voltage of mains frequency can also be applied to the horizontal deflecting system or to both systems. In the first case the so-called Lissajous curves are obtained and in the second case ellipses, which may be seen on the screens in figs. 2 and 3.

Fig. 4c shows a section through the electrical portion of the demonstration model, which consists of a radio receiver with 53 auxiliary units. This part (see *fig. 6*) is enclosed in a metal chamber which effectively screens off the action of surrounding disturbing fields. (A tramway line with heavy traffic passed directly under the Philips stand at the exhibition.) As the sand figures require a considerable amount of space and the cathode ray tubes must also not be placed too close to each other, the whole model is 7.5 metres long and is thus probably the largest radio receiver in the world. The demonstration model was constructed in the Research Laboratory on designs of R. P. Wirix.

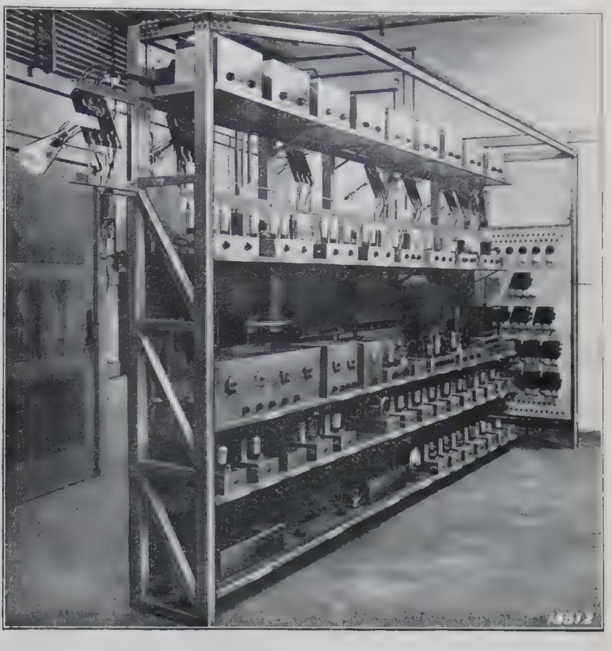

Fig. 6. Rear view of model.

Compiled by H. J. J. BOUMAN.

---

[1]) For the time-base deflection the saw-tooth variation of a special type of relaxation oscillations is employed. For further details see: Philips techn. Rev. 1, 16, 1936.

# ABSOLUTE SOUND-PRESSURE MEASUREMENTS

By J. DE BOER.

**Summary.** The paper discusses two methods for the measurement of sound pressures, by both of which a microphone is calibrated. The difference of the results is within the limits of discrimination of the ear.

## Introduction

To determine the sensitivity of a loudspeaker or a microphone it is necessary to measure two magnitudes of different quality, an electrical magnitude (e.g. the current passing through the coil of the loudspeaker or the voltage at the output terminals of the microphone) and an acoustic magnitude (e.g. the sound output of the loudspeaker or the sound pressure at the location of the microphone). The first two sections of this article describe two methods for measuring sound pressures. In the first Raleigh's disc is used and in the second the condenser microphone. In the concluding section details are given of the results of a calibration carried out by these two methods.

## Raleigh's Disc

Raleigh's disc is a thin circular plate suspended from a torsion wire (*fig. 1*). If a disc of this type hangs vertically in a uniform or periodic stream of gas or fluid, it will sustain a torque which will tend to turn its surface in a direction perpendicular to the direction of flow. The magnitude of this torque $M$ is determined by the mean velocity $v$ of the vibrating air particles. If $M$ is known then the velocity and hence also the sound pressure can be calculated. Rayleigh was the first to investigate these phenomena. König 1) has calculated the torque $M$ on the basis of the following assumptions:

a) An incompressible fluid,
b) uniform rate of flow, and
c) total absence of friction and viscosity.

He obtained the expression:

$$M = \frac{4}{3}\, \varrho\, a^3\, v^2\, \sin 2\vartheta \qquad (1)$$

where $\varrho$ is the density of the fluid, $v$ the velocity of flow, $\vartheta$ the angle between the vertical to the disc and the direction of flow, and $a$ the radius of the disc.

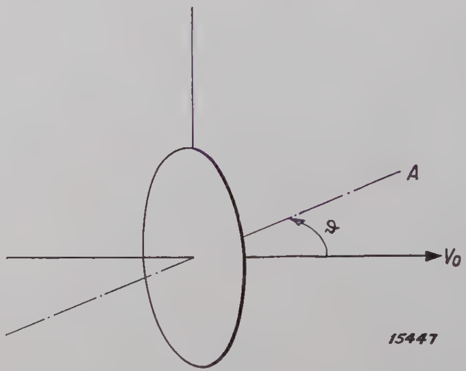

Fig. 1. Rayleigh's disc. The atmospheric vibrations in the field of sound exercise a torque on the disc such that its axis $A$ tends to turn into the direction of propagation $v_0$ of the sound. The torque has its greatest value when the angle $\vartheta$ between $A$ and $v_0$ is 45 deg.

With the aid of the streamline diagram reproduced qualitatively in *fig*. 2, an idea may be gained of the action of the flowing medium on the disc. With a current flowing in a horizontal direction without eddies, the following relationship connects the pressure $p$ and velocity $v$:

Pressure energy + kinetic energy = constant.

Applying the theorem to 1 cm³ of the fluid gives Bernoulli's equation:

$$p + \frac{\varrho}{2}\, v^2 = \text{constant.}$$

The highest excess pressure $p_m$ is obtained at the condensation points $P_1$ and $P_2$ in fig. 1, where the velocity of flow is zero. The peak values of the pressure on the back and front of the disc are obviously displaced with respect to each other and produce a torque which tends to turn the disc perpendicular to the direction of flow. If the pressure distribution on the front and rear of the disc is in each case replaced by the resultant $K$, one obtains *fig*. 3. It is clear that

the pressure $p$ is proportional to $^1/_2\, \varrho\, v_0^2$,

the force $K$ is proportional to $^1/_2\, \varrho\, v_0^2\, \pi\, a^2$,

The torque $M$ is proportional to $^1/_2\, \varrho\, v_0^2\, \pi\, a^2\, a$.

This result is in agreement with equation (1). Furthermore it is obvious from conditions of symmetry that the torque must disappear if the angle between the disc and the direction of flow is either zero or 90 deg. This is expressed by the term *sin* $2\vartheta$ in equation (1).

For the purpose of König's calculation it is not absolutely essential to assume that the flow is uniform. Equation (1) also applies to periodically-variable conditions of flow provided the wave-length is sufficiently great compared with the dimensions of the disc. The mean value of the torque is therefore:

$$\overline{M} = \frac{4}{3}\,\varrho\, a^3\, \overline{v}^2 \sin 2\vartheta \qquad (2)$$

where $\overline{v}^2$ is the mean square of the velocity. $\overline{M}$ represents the torque produced by a sound field 1). As owing to its inertia Raleigh's disc cannot respond to acoustic vibrations, the average torque alone is of practical interest. From equation (2) one gets:

$$\overline{v} = \sqrt{\frac{3\,\overline{M}}{4\,a^3\,\varrho \sin 2\vartheta}} \qquad (3)$$

By carrying out a measurement of $\overline{M}$, $\overline{v}$ can be calculated from this equation, i.e. the square root of the mean square velocity of the vibration. The relationship between $\overline{v}$ and the corresponding sound pressure $\overline{p}$ depends on the type of sound waves under consideration.

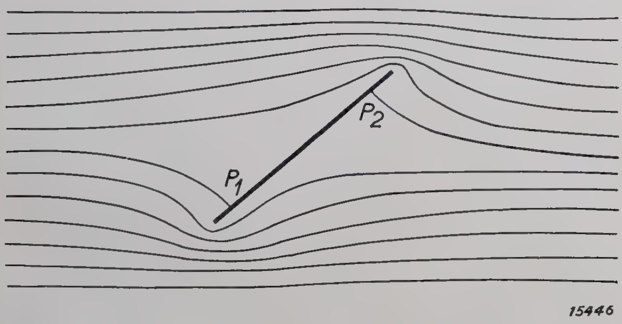

Fig. 2. Streamlines around an infinitely long strip arranged perpendicular to the plane of the paper. The diagram also applies qualitatively for the conditions of flow round a circular disc. The hydrodynamical pressure is greatest at the condensation points $P_1$ and $P_2$.

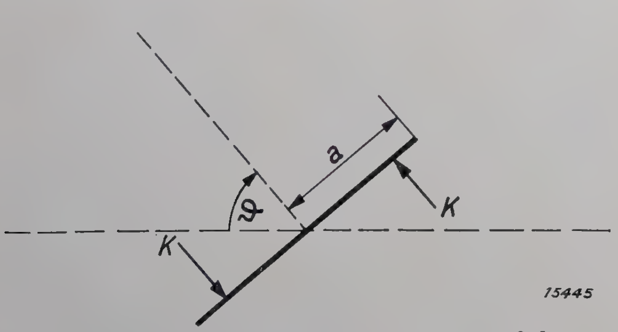

Fig. 3. Hydrodynamical forces. The resultants $K$ of the component pressures on the rear and front sides of the disc are displaced with respect to each other (corresponding to the positions of the condensation points) and produce a torque. The arm on which this torque acts is proportional to the radius $a$ of the disc; the force $K$ is proportional to the surface area $\pi a^2$ of the disc.

With plane waves, this relationship is expressed by $p = \varrho \cdot c \cdot v$, where $c$ is the velocity of sound. If $c$ is measured in cm per sec, we get for air at 1 atmospere pressure and a temperature of 20 deg. C numerically:

$$\overline{p} = 42{,}6\ \overline{v}\ \mathit{bar} \ \text{(see footnote 2))} \qquad (4)$$

In the case of spherical waves emitted from a point source of sound, the relationship between the sound pressure and the velocity of the vibrating particles is by no means so simple. For a sound with a frequency $\nu$ and a wave number $k$ (i.e. $k$ wave-lengths per unit of length) the laws ruling $p$ and $v$ take the form:

$$p = A \sin 2\pi (\nu t - kr)$$

$$v = A \cdot \varrho \cdot c \left[ \sin 2\pi(\nu t - kr) - \frac{\cos 2\pi(\nu t - kr)}{2\pi kr} \right]$$

These expressions indicate that equation (4) is applicable also to spherical waves with an accuracy of $1\ {}^0/_{00}$, if the distance $r$ from the source of sound is at least 3.5 wavelengths of the sound under consideration (e.g. 120 cm with 1000 cycles).

Deviations from König's theory occur, when the length of the sound waves becomes comparable with the diameter of the disc. If the disc has a diameter of 1 cm, the correction required at 10,000 cycles is in the neighbourhood of 10 per cent.

## Measurement of the Torque

The torque $\overline{M}$ given by equation (2) will turn the disc through an angle $\alpha$, which will have such a magnitude that the elastic strain of the torsion wire will balance the torque ($\overline{M} = D\,\alpha$). The angular deflection $\alpha$ of the reflecting disc is determined by the reflected beam method, which consists in viewing through a telescope the image of a scale reflected by the disc (see fig. 4). The directing torque $D$ is obtained from the time of oscillation $T$ of the disc when swinging freely and from its known moment of inertia $Q$, thus:

$$D = \frac{4\pi^2 Q}{T^2}; \quad M = \frac{4\pi^2 Q}{T^2}\,\alpha \qquad (5)$$

Substituting $M$ in equation (3), we get the average velocity:

$$\overline{v} = \frac{\pi}{T}\sqrt{\frac{3\,Q\,\alpha}{\varrho\, a^3 \sin 2\vartheta}} = \frac{5{,}44}{T}\sqrt{\frac{Q\,\alpha}{\varrho\, a^3 \sin 2\vartheta}} \qquad (6)$$

---

1) The medium of the sound-waves does not correspond with the assumption of an incompressible frictionless fluid as made by König in his calculations. Nevertheless, as King II) has shown, König's result as summarised in equation (1) also applies to sound-waves.

2) 1 bar = 1 dyne/sq.cm. = $0.75\ 10^{-3}$ mm Hg.

Equation (6) expresses the velocity $\bar{v}$ of the sound vibrations as a function of the angular deflection $\alpha$ of Raleigh's disc. All other terms in the equation are known.

It suggests itself that these measurements could be suitably carried out in the open air where no reflected sound would be a source of disturbance. This, however, has proved impossible as Raleigh's disc responds, not only to audio-frequency sound waves, but also to slowly-variable air currents which always occur with measurements in the open and seriously disturb measurements, due to the long oscillation time of the disc. For this reason the disc was suspended in a room surrounded by walls having a high sound-absorption factor (*fig. 4*). The wall opposite the sound-source was left open as it is the sound-wave reflected from this wall which constitutes the most serious source of error. The higher the frequency, the lower is the interference due to reflected waves, since the absorption coefficient of the walls increases with the frequency and since, moreover, if a loudspeaker is the source of sound, the beam of sound becomes increasingly directional with rising frequency.

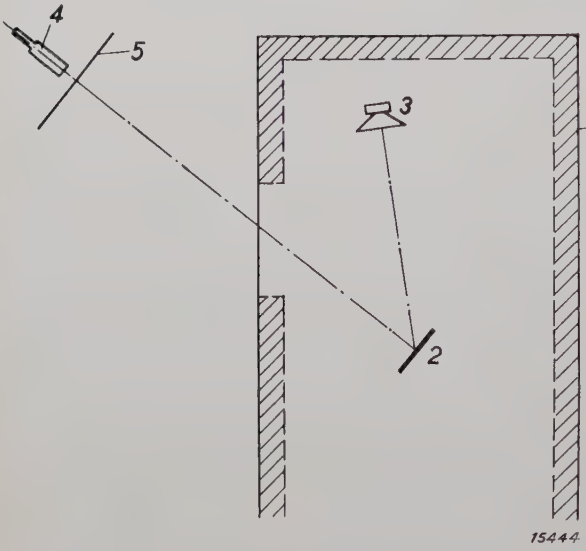

Fig. 4. Room with sound-absorbing walls suitable for measurements with Rayleigh's disc.

1. Wall covering
2. Rayleigh's disc
3. Loudspeaker
4. Telescope
5. Scale.

### The Condenser Mikrophone

The responsive element of the condenser microphone is a diaphragm conducting electricity **1** (e.g. of aluminium 20 $\mu$ in thickness), stretched directly in front of an electrode **2**. This diaphragm vibrates under the action of the sound-waves in exact response to the fluctuations in pressure. The capacity of the condenser composed of the electrodes **1** and **2** is thus subject to a periodic fluctuation. As the condenser is charged, the fluctuations in capacity become converted into fluctuations in voltage, which are measured by means of an amplifying voltmeter. The circuit of the condenser microphone and its connection with the first valve of the voltmeter is shown in *fig. 5*.

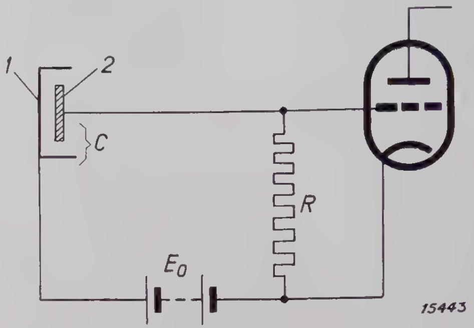

Fig. 5. Diagrammatic sketch of a condenser microphone.

**1** = Diaphragm
**2** = Contra-electrode
$R$ = Resistance leak
$E_0$ = Battery.

The varying sound-pressure acting on the diaphragm **1** produces changes in the capacity $C$. As a result the voltage of the condenser fluctuates, since the charge cannot flow with sufficient speed from or to the condenser via the resistance $R$.

If $\omega$ is the angular frequency of the sound, the distance between the electrodes **1** and **2** can be expressed by:

$$d = d_0 - d_1 \sin \omega t$$

where $d_o$ is the mean value of the distance between the plates and $d_1$ is the amplitude of oscillation. The capacity $C$ of the condenser is also subject to periodic variation:

$$C = \frac{\text{Surface of plates}}{4 \pi \cdot \text{gap}} = \frac{O}{4 \pi (d_0 - d_1 \sin \omega t)}$$

At a sufficiently low frequency, a quantity of electricity would flow either to or from the condenser through the resistance $R$ such that the E.M.F. of the condenser would remain constant, viz, equal to the battery voltage $E_0$. At sufficiently high frequencies (time of oscillation small as compared with the relaxation time $RC$ of the condenser [3]) the charge $q$ of the condenser may, however, be regarded as invariable ($q = OE_0/4 \pi d_0$). The E.M.F. of the condenser then becomes:

$$U_C = \frac{q}{C} = \frac{q}{O} 4\pi (d_0 - d_1 \sin \omega t)$$

---

[3] The period of discharge of a condenser $C$ through a resistance $R$ is given by the product $RC$ (cf. the article dealing with relaxation oscillations, this journal **1**, 44, 1936).

The potential difference $U_R$ across the terminals of $R$ is:

$$U_R = E_0 - U_C = \frac{4\,\pi\,q}{O}\,d_1\,\sin\,\omega\,t$$

$$= E_0\,\frac{d_1}{d_0}\,\sin\,\omega\,t \qquad (7)$$

As stated above, equation (7) applies when

$$RC \gg \frac{1}{\omega} \text{ or } RC\,\omega \gg 1.$$

In order to draw conclusions regarding the sound pressure from the amplified alternating voltage, the elastic characteristics of the diaphragm must be known and in addition all other magnitudes in the electrical amplifier. The very tedious work of determining the numerical value of each factor can, however, be dispensed with, since the whole system can be calibrated by applying a known pressure, generated electrically. This pressure is generated by means of an electrode placed in front of the diaphragm. Applying to the fronting electrode the sum of a D.C. voltage and an A.C. voltage of audio-frequency, the diaphragm will be attracted by alternating forces which can be easily calculated.

The tension on the plate of a condenser is:

$$p = \frac{E^2}{8\pi}$$

where $E$ is the electrical field-strength. In the case in question (*fig.* 6) $E = E_1 + E_2 \sin\,\omega\,t$ and hence

$$p = \frac{1}{8\,\pi}\left[E_1^2 + 2\,E_1\,E_2 \sin\omega t + {}^1\!/_2\,E_2^2\,(1 - \cos\,2\omega t)\right] \qquad (8)$$

The pressure expression contains a constant term, a term which varies with the angular frequency $\omega$ and a term varying with $2\,\omega$. It is therefore not purely harmonic, but also includes a second overtone. This latter can, however, be neglected if the amplitude $E_2$ of the A.C. voltage is sufficiently small with respect to $E_1$. If $E_1$ is zero, only the overtone is obtained, i.e. a purely harmonic oscillation of double the frequency.

The fronting electrode (fig. 6) is designed as a latticed bar. If a solid plate were used an enclosed air-space would be produced between 1 and 3, and as a result the diaphragm would acquire an additionall stiffness during calibration which would be absent in ordinary sound-pressure measurements. As the above calculation of the sound pressure applies to a flat electrode, equation (8) is not strictly correct, and there should be included a correction factor independent of the frequency [III]).

In measurements with the condenser microphone two further corrections must still be taken into account, for the microphone measures the sound-pressure at the location of the diaphragm, while actually information is required of the pressure at the same point in the absence of the microphone. For two reasons the pressure is not the same in the absence and presence of the microphone:

a) Owing to refraction of the sound-waves around the microphone, a phenomenon which increases the sound pressure. The smaller the wave-length of the sound, the greater will be this correction. If the sound-waves are small compared with the diameter of the diaphragm, the sound-pressure will be doubled. The requisite correction can be calculated if the design and dimensions of the microphone are known [IV]).

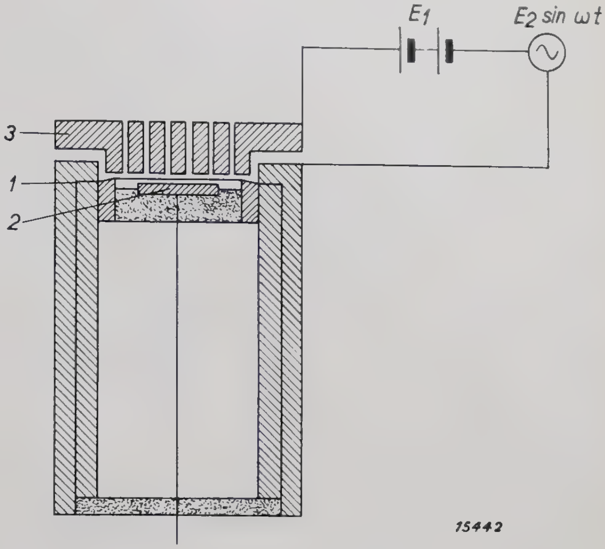

Fig. 6. Section through a condenser microphone with electrode placed in front of it.

**1** = Diaphragm
**2** = Contra-electrode
**3** = Fronting electrode.

By means of a D.C voltage ($E_1$) and an A.C. voltage ($E_2 \sin \omega t$), connected in series to the fronting electrode, a pressure of known magnitude and frequency is applied to the diaphragm. Bij this means the whole system can be calibrated.

b) Owing to the shape of the housing. The microphone is designed in such a way that the diaphragm

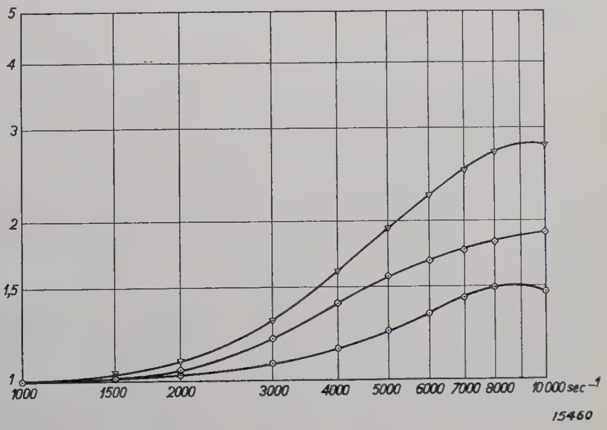

Fig. 7. Correction factors for the condenser microphone. Lower curve: Correction for resonance of the extension, mean curve: Refraction correction, upper curve: Total correction.

With sound-frequencies of 10,000 cycles the pressure on the diaphragm is nearly 3 times as great as the pressure at the corresponding point in space in the absence of the microphone At frequencies below 1000 cycles no corrections need be made.

constitutes the rear of a short cylindrical extension tube. The pressure on the diaphragm is not exactly equal to the pressure on the front surface of the extension. Ballantine and West have calculated the ratio of the two pressuresV). In *fig. 7* in addition to the correction for refraction, computed for a microphone of 25 mm diameter, the correction due to the resonance of the extension tube is also shown as a function of the frequency for an extension 3 mm long, and a diaphragm 18 mm in diameter. The upper curve in this figure represents the aggregate correction taking into consideration these two factors.

### Measurements with the Condenser Microphone

As already pointed out, the voltage of the microphone is amplified. The amplifier must not be placed too close to the microphone as otherwise it will interfere with the field of sound. On the other hand the leads from the microphone to the amplifier must not be too long, since otherwise the capacity of the leads becomes too high.

The method is particularly suitable for use in the open air. The effect of uniform air currents can be neglected, and although sudden air impulses do affect the deflection, these can be readily detected, since the voltmeter operates with practically no lag.

### Comparison of the Two Methods

A Raleigh disc was suspended in front of a loudspeaker at a distance of 1 m. The loudspeaker current was adjusted for different frequencies such that the disc indicated a sound-pressure of 1 bar. A condenser microphone was then substituted for the Raleigh disc and the voltage at the output terminals of the microphone amplifier was measured with exactly the same frequencies and current intensities through the loudspeaker coil. The calibration curve for the microphone obtained in this way was compared with electrostatic calibration results, allowing for the corrections discussed above. The result obtained is shown in *fig. 8*.

The degree of concordance between the two methods is entirely satisfactory. Throughout the whole frequency-range up to 8000 cycles the results differ by less than 7 per cent (i.e. by less than 0.6 db 4)). At very low frequencies the Rayleigh disc is perhaps slightly less reliable, for the effect of the reflected waves is difficult to eliminate in these circumstances. On the other hand, at the highest frequencies less credence must be put on the indications of the condenser microphone, as the corrections for refraction are then very large (e.g. at 8000 cycles almost equal to a factor 3). The maximum difference of 7 per cent between the two methods is below that which can be detected by the human ear. The degree of accuracy thus conforms with all practical requirements.

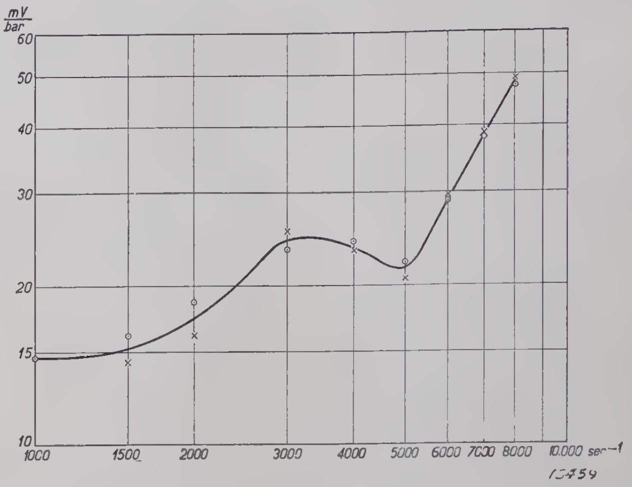

Fig. 8. Calibration of a condenser microphone. Sensitivity of the microphone in millivolts per bar plotted as a function of the frequency.
× Calibration by means of the fronting electrode
⊙ Calibration by means of Rayleigh's disc.

## LITERATUUR

I) W. König, Wied. Ann. **43**, 43, 1891.
II) L. v. King, Proc. Roy Soc. **A. 153**, 17, 1935.
III) S. Ballantine, Journ. Ac. Soc. Am. **3**, 352, 1932.
IV) S. Ballantine, Journ. Ac. Soc. Am. **3**, 319, 1932.
V) S. Ballantine, Proc. I.R.E. **18**, 1206, 1930.
W. West, Proc. Inst. Electr. Eng. **5**, 145, 1930.

---

4) The difference $\Delta I$ of two sound-intensities corresponding to the sound-pressures $P_1$ and $P_2$, is defined by $\Delta I = 20 \log_{10} P_1/P_2$ decibel. The ear cannot discriminate differences below 1 decibel, i.e. of 12 per cent of the sound-pressure.

# HIGH-FREQUENCY OSCILLATIONS IN SODIUM LAMPS

By L. BLOK.

**Summary.** In addition to the high-frequency oscillations occurring on ignition with all discharge tubes fed with alternating current, permanent high-frequency oscillations can also be present in the discharge in sodium lamps, and in certain circumstances, if no suitable precautions are taken, these can interfere with radio reception. The investigation of these oscillations in direct-current lamps has resulted in the recognition of two types of oscillations, A and B, which differ from each other in their external characteristics and in their response to several factors. Type A oscillations are apparently due to oscillations of positive ions, and type B to oscillations of electrons. With current designs of lighting equipment, in which each lamp is fed via its own auto-transformer (with secondary winding split into two parts symmetrically connected to the lamp), the oscillations normally do not react on the mains supply. In special cases where interference with radio reception may occur, a small and simple interference suppressor will be found adequate to remove all interference.

## Introduction

It is well known that in discharges through gases high-frequency oscillations may occur, which by radiation or transmission along conductors may cause interference with radio receiving apparatus in the neighbourhood. The propagation of these oscillations to the mains supply is nowadays in the case of sodium lamps avoided very simply by a suitable design and circuit for the supply transformer. In order to find out what precautious would be suitable for avoiding interferences, it was desirable to obtain a closer insight into the production and nature of these oscillations.

A distinction must here be drawn between high-frequency oscillations generated during the burning of the lamp and those generated during ignition. The latter type is a well-known cause of radio interference; it may occur with practically all A.C.-fed discharge tubes, such as the neon tubes used in luminous signs, rectifying valves, etc., which are started up and extinguished again twice in each period. In many cases this kind of interference is absent altogether; when it occurs, however, it is similar to the interference caused by sparking at switches and electric motors. An analysis of this type of oscillation offers no new information and will therefore not be discussed here, the more so since these oscillations are rendered harmless by interference suppressors at the same time as the oscillation of the gas discharge per se.

In the case of interference from direct-current discharges it is evident that only the permanent high-frequency oscillations can be responsible, for ignition only takes place once here, viz, on switching on. That the permanent oscillations may in certain circumstances interfere with radio reception was seen on adopting sodium lamps (which were originally of the D.C. type) for street lighting. This gave the impetus to a closer investigation of the problem, the results of which are briefly outlined in this article 1).

## Measurement of the High-Frequency Oscillations

At the outset an arrangement was evolved for measuring the high-frequency oscillations. The apparatus used for outdoor measurements consisted of a transportable receiver with aerial, the high-frequency oscillation being reproduced in the loudspeaker as a radio interference, while at the same time the rectified voltage was measured with an

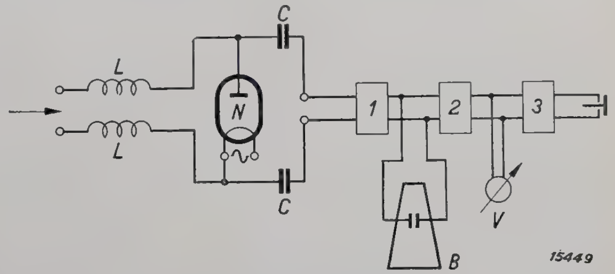

Fig. 1. Measuring apparatus for investigating high-frequency oscillations in sodium lamps. The lamp $N$ is fed with direct current. Two chokes $L$ prevent the transmission of the high-frequency oscillations to the network, and two condensers $C$ shut off the unidirectional voltage from the actual measuring apparatus. *1* is a high-frequency amplifier, behind which the cathode-ray tube $B$ is connected. In 2 the high-frequency oscillations are rectified and in the amplifying voltmeter $V$ connected after it the high-frequency voltage is measured. 3 is a low-frequency amplifier which renders the oscillations audible in the loudspeaker as radio interference.

---

1) Although, in the meantime, the Philips Works have for various reasons changed over to the production of sodium lamps for alternating current, the observations made on direct-current lamps are still of interest.

amplifying voltmeter. In measurements in the laboratory the high-frequency voltage was in addition rendered visible by means of a cathode-ray tube. For this purpose, however, the high-frequency oscillation was tapped directly from the lamp. The experimental apparatus used is shown in *fig. 1*.

By means of a band-pass filter in the high-frequency amplifier, various wave-bands from 200 to 2000 m could be adjusted for determining the frequency range of the oscillations. The fluorescent spot on the screen of the cathode-ray tube was expanded to a luminous line of adjustable length (time axis), by means of a "saw-tooth" deflection voltage [2]). The (amplified) high-frequency voltage broadened this line to a band (*fig. 2*) whose width was a direct measure of the amplitude of this voltage. In subsequent measurements with A.C. lamps the time-deflection frequency was synchronised with the frequency of the A.C. mains supply or with a fraction of this frequency; in this way information was also obtained of the distribution of the oscillations throughout the period of the A.C. supply.

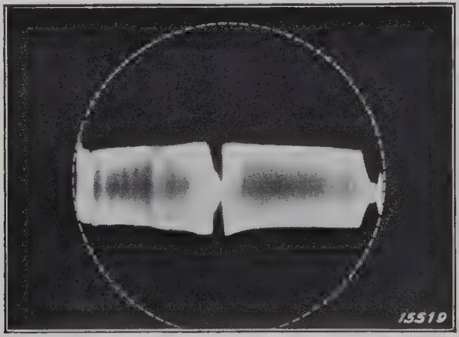

Fig. 2. Fluctuation of the high-frequency voltage of an alternating current sodium lamp ("Philora" type SO 100) during a single period of the mains alternating current. The fluorescent spot on the screen of the cathode-ray tube is elongated to a (horizontal) luminous line, the time-axis, by a "saw-tooth" voltage. The high-frequency voltage deflects the electron beam in a direction perpendicular to the time axis, and the luminous line of the fluorescent screen is broadened to the band photographed here. The width of the band is a measure of the amplitude of the high-frequency voltage. The time-deflection frequency is synchronised with the frequency of the A.C. mains supply. If conditions are exactly the same in each period, a stationary image is obtained. Exposure time of this picture was about 10 periods (approximately $^1/_5$ sec).

The majority of the measurements made were carried out with sodium lamps of the low-voltage arc type. These lamps were fed with 24 volts unidirectional current (the voltage drop was approximately 14 volts). The arc intensity $i_b$ was 5 to 12 amps, the cathode was heated by an alternating current $i_f$ of about 10 amps.

## Two Types of Oscillation

The oscillations obtained with different lamps were never of exactly the same type. Yet it was soon established that two essentially different types of oscillation A and B were present, providing criteria by which almost all lamps could be classified according to their behaviour.

Type A oscillations contain components with frequencies from about $1.5 \cdot 10^6$ to $0.5 \cdot 10^6$ cycles corresponding to wave-lengths $\lambda$ of 200 to 600 m. The components are found to be at certain fairly well-defined wave-lengths in this range. In many cases the frequency difference between several successive components was constant, and these may therefore be regarded as harmonics of an oscillation of much lower frequency (i.e. equal to the frequency difference in question, with $\lambda$ up to 30,000 m), whose existence was proved indirectly in this manner. Type A oscillation is modulated to a marked degree with the frequency of the heating current (50 cycles).

Type B oscillations are also situated in the range of wavelengths from 200 to 600 m, but cover a more continuous frequency band. They are much weaker than A and cannot therefore be detected by the oscillograph; they are modulated to a lesser degree or not at all. The striking observation was made that in suppressing radio interference due to the B type of oscillation (but not of the A type) by means of a condenser connected in parallel (see below), the length of the connecting leads played an important part. It may be concluded from this that the B oscillations also contain an ultra-short wave component.

More striking still than the difference in the characteristics of these types of oscillations is their difference in response to conditions under which the lamp is run. The determining factors here are the arc intensity $i_b$ and the intensity of the heating current $i_f$; $i_b$ determines the concentration of the ions in the discharge and $i_f$ the emission of electrons from the cathode [3]). If a lamp generates type A oscillations, oscillation increases as $i_b$ is raised and/or $i_f$ is reduced. If on the other hand the lamp is subject to B oscillations, its behaviour is the exact converse: oscillation increases as $i_b$ is reduced and/or $i_f$ is increased. In very many lamps a transition from type A to type B could in fact be obtained by altering $i_b$ and $i_f$. In a lamp with A oscillations, by reducing $i_b$ and raising $i_f$, the amplitude of the high-frequency voltage (read on the amplifying voltmeter) was progressively reduced, and eventually disappeared altogether at certain values of $i_b$ and $i_f$; on a further alteration of $i_b$ and $i_f$ in the same sense, type B oscillations then made their appearance with a gradually increasing amplitude. In principle this could provide a means for eliminating a possible radio interference, viz, by suitable regulation of the arc and heating currents of the lamps. In practice, however, this method of suppression is not suitable. Even if the working conditions of the lamp were not already fixed by other considerations, and the transition from type A to type B could be effected in all lamps via an intermediate state devoid of oscillation (which is definitely not the case), a single regulation of each lamp would not in fact suffice, since the oscillatory behaviour of the lamps varies considerably with increasing age. Moreover, the oscillations can be rendered harmless by much simpler means, as is shown below.

---

[2]) See e.g. Philips techn. Rev. 1, 19, 1936.

[3]) Actually the emission of electrons is also determined by $i_b$, as the ions may pull out extra electrons from the cathode and also may heat the cathode by their bombardment. On a variation of $i_b$, there is thus a change in the concentration of the ions as well as in the emission of electrons.

As already pointed out, type A oscillations are promoted by an increase in the ion concentration and reduced emission of electrons, while type B oscillations are promoted by just the opposite, viz, an increase in emission and a reduced ion concentration. These facts suggest that in the case of type A oscillations the oscillations of positive ions in the discharge play a part, while with type B on the other hand the oscillations of electrons are the governing factor. Oscillations of ions and electrons in gases have in fact been known for some time. The frequencies which have been deduced theoretically for the oscillations of ions are also of the same order of magnitude as those found here. The oscillation of electrons may perhaps be regarded as a Barkhausen-Kurz oscillation [4]) in which the positive space-charge cloud hovering behind the cathode fall assumes the rôle of the positive grid [5]).

## Suppression of Oscillations

Investigation of the high-frequency oscillations obtained with various street-lighting systems confirmed the results of laboratory work. In particular it was found that an overhead feeder system with a number of sodium lamps connected in series selected from the wide frequency-band of the lamps' oscillations the particular frequency to which it was "tuned". Along the feeder stationary waves are produced, whose nodes and antinodes may be readily located by moving the transportable measuring equipment along the feeder. Hence from the point of view of the feeder promoting interference, a lighting system fed through a buried cable is more suitable than an overhead feeder owing to the smaller amount of radiation due to the cable. With the latter an ordinary interference filter may prove sufficient to prevent the propagation of the high-frequency oscillations to other sections of the supply.

At the present day, however, it is more common practice to connect the lamps in parallel than in series. In these systems interference is suppressed in the following way. Each lamp is connected in parallel to the supply via its own auto-transformer (*fig. 3*). For both lamp terminals a portion of the secondary winding of the transformer acts as a choke, which prevents the propagation of the high-frequency oscillations. All interferences are avoided by this arrangement, provided the transformer is placed directly next to the lamp. Where this is not possible, for instance in cases where the lamp and transformer are separated by a section of the overhead feeder (acting as an aerial), each lamp must be supplemented by its own suppression units. This is done in the usual way by the addition of condensers and self-induction coils.

For direct-current lamps, a small condenser of about 2 μF rating is in general sufficient for suppressing the high-frequency oscillations. To ascertain whether a lamp is oscillating or not, a simple method was available here. The voltage-drop across the lamp is measured, the condenser being paralleled during measurement. If high-frequency

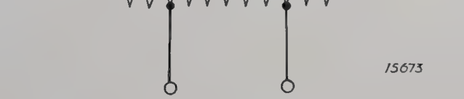

Fig. 3. Current method of interconnection of lamps for suppressing high-frequency oscillations. Each lamp $N$ is connected in parallel to the mains with its own auto-transformer $T$, in such a way that a portion of the secondary winding of the transformer acts on the two poles of the lamp as a high-frequency choke, thus preventing the propagation of the high-frequency oscillations to the network. The magnetic characteristics of the transformer, which for the sake of simplicity have not been shown here, are in fact of essential importance in the high-frequency choke-action.

---

[4]) These are oscillations of very high frequency ($\lambda = 10$ to 100 cm) which may occur in a radio valve if the grid is given a high positive voltage with respect to the anode.

[5]) See F. M. Penning, Physica **6**, 241, 1926.

oscillations of type A are being generated this voltage-drop will increase a little at the instant the condenser is connected up, i.e. at the moment the oscillations cease. As a result of these oscillations the requisite number of ions is apparently already generated at a somewhat lower average voltage. If the high-frequency voltage fluctuations disappear owing to the elimination of the oscillation, a higher (now constant) working voltage must be attained to reproduce the same number of ions. Type B oscillations cannot be detected by means of this effect. But experience has shown that direct-current lamps, which at the moment give type B oscillations or do not oscillate at all, steadily pass over to type A oscillation with increasing age [6].

In the case of alternating-current lamps it is not permissible to connect a condenser of the rating indicated in parallel with the lamp, as the impulses in the discharge resulting therefrom would increase flickering; moreover, the working life of the tubes would be reduced owing to the high instantaneous values of the current densities. In these lamps, therefore, in order to render the external effect of the high-frequency alternating voltage $E$ harmless, a self-inductance $L$ of about 4 millihenries and a condenser $C$ of approximately 0.01 $\mu$F rating are provided in the manner shown in *fig. 4*. With the chosen values of $L$ and $C$ we have $\omega L >> 1/\omega C$, so that the high-frequency current in the $LC$ circuit is approximately $i = E/\omega L$ and the interference voltage reacting on the rest of the system (being equal to the potential of the condenser) is $e = E/\omega^2 LC$. The interference-suppression factor obtained in this way is therefore $E/e = \omega^2 LC$ (for the smallest frequencies coming into question $E/e$ is approximately equal to 30).

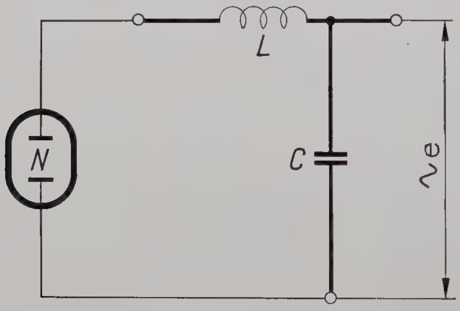

Fig. 4. Suppression of interference in alternating-current lamps by means of a self-induction coil $L$ connected in series and a condenser $C$ connected in parallel. The suppression factor is $\omega^2 LC$.

*Fig. 5* reproduces a photograph of the interference-suppression unit in which the condenser and the self-induction coil are combined; it can be connected without preliminary alterations to any lamp where suppression is considered desirable. *Fig. 6* shows a lighting fitting with the suppressor unit incorporated.

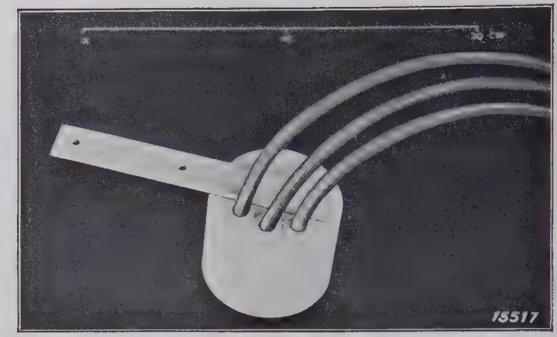

Fig. 5. Photograph of the small interference-suppression unit. The three wires are connected up in the manner shown in fig. 3.

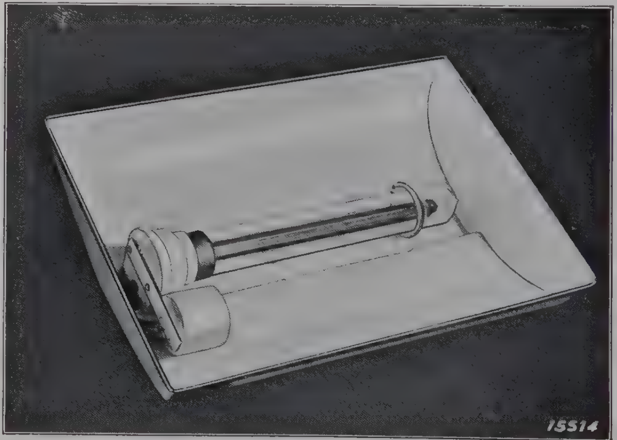

Fig. 6. Lighting unit with interference-suppression unit (left) incorporated.

---

[6] This is probably connected with the gradual reduction in emission of the cathodes (corresponding to a reduction in $i_f$).

# CONTROL OF THE BEAM INTENSITY IN CATHODE RAY TUBES

**Summary.** A survey is given of the principal methods which have been devised for the control of the current intensity in cathode ray tubes. Characteristics of the Philips cathode ray tubes 3951/3952 are discussed.

## Introduction

In the preceding issue of this Review[1]) the production of high-definition fluorescent spots in cathode ray tubes was discussed, but the brightness of the light-spot on the fluorescent screen was not then dealt with in detail. In general it is unnecessary to regulate the intensity of the beam in cathode ray oscillographs, but where these oscillographs are used for television reception, fluctuation in the brightness of the picture spots due to variations in the beam intensity has a considerable bearing on the definition of the picture [2]). For sound-films a procedure (Lignose-Breusing) is elaborated in which a cathode ray tube is used where the electron beam is not deflected but only varied in intensity. The fluorescent spot on the screen is photographed on the film and its varying brightness is used in this manner for registration of the sound. In the present article the principal methods for controlling the beam intensity will be discussed in some detail.

The brilliancy of the bright spot on the screen is determined by the current density of the electrons which produce the spot, and by their velocity. When it is required to alter the intrinsic brilliance of the spot, but without in any way affecting its size and position on the screen, it is sufficient to change the velocity of the electrons by varying the accelerating field (voltage modulation) while keeping the current intensity constant. In television receivers it is imperative that a change in intensity does not produce any alteration whatsoever in the size of the picture spot or its position on the screen. As this condition is extremely difficult to be satisfied by voltage modulation, the usual method employed in cathode ray tubes for television reception is to vary the current intensity of the electron beam, but to leave unchanged the voltages for accelerating and deflecting the beam (so-called current or intensity modulation). The intrinsic brilliance of the fluorescent spot is proportional to the current intensity within the range of current densities employed in television reveivers.

The deflection response of the electron beam is not affected by intensity modulation. The spontaneous concentration of the beam in gasfilled tubes due to the space-charge of the positive ions is, however, dependent on the current intensity. As already indicated in the previous issue [3]), gasfilled cathode ray tubes have only a limited application for television purposes for this very reason.

### Current or Intensity Modulation

Since the intensity of the electron beam must frequently be altered very rapidly, it is not possible to vary the current intensity by regulating the heating current of the cathode. The emission temperature, and hence also the emission current, is too slowly built-up for this method to be of use. Mechanical control of the current (e.g. by means of an adjustable screen) would also possess too great an inertia (in television apparatus modulation frequencies of the order of $10^6$ cycles are met with).

There are nevertheless available two fundamentally different methods of electrical current modulation which operate with a sufficiently low inertia.

1. A variable part of the electron beam is passed through a screen, by imparting to the beam in front of the screen a small variable deflection.

2. A variable portion of the electrons emitted is forced back to the cathode by applying a variable opposing field in the immediate neighbourhood of the cathode.

### Current Modulation with Screen

The electron beam is pre-concentrated by means of a Wehnelt cylinder. As long as no potential is applied to the plates $P$ and $P'$ almost all the electrons pass through the small aperture in the centre of the anode $A$. The shape of the beam where $P$ and $P'$ have a positive bias with respect to the anode is shown in *fig. 1.* A portion of the beam which increases as the voltage is raised is cut off by the edge of the screen. The deflections of the electron beam produced by the plates *P* and *P'* balance each other, so that the spot is not appreciably displaced on altering the intensity.

---

[1]) Philips techn. Rev. **1**, 33, 1936.

[2]) See J. van der Mark, Philips techn. Rev. **1**, 16, 1936. In addition to intensity control, velocity regulation is also employed for television purposes and consists in passing an electron beam of constant intensity over the various parts of the picture at a high speed varying with the latter's brightness. Space does not permit this method to be discussed in detail in this article.

[3]) Philips techn. Rev. **1**, 38, 1936.

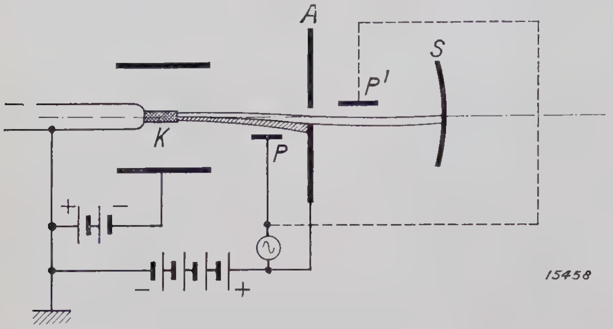

Fig. 1. Current modulation by deflection of the ray, using the electrode *P*. The electrode *P'* compensates the deflection so that the light-spot is not displaced on the screen.

Instead of unilateral screening of the electron beam by the edge of the aperture, the ray can also be symmetrically screened off on all sides. An arrangement for doing this is illustrated in *fig. 2.* By applying an alternating potential between the cathode and the cylinder *C*, the focussing action of the cylinder can be varied in such a way that a variable fraction of the electron beam passes through the aperture in the screen. This arrangement has the disadvantage that the definition of the spot is influenced by modulation, since the distance of the cathode image varies with the potential applied to *C*, but can be avoided by throwing on the fluorescent screen not an image of the cathode but an image of the screen aperture at *A*.

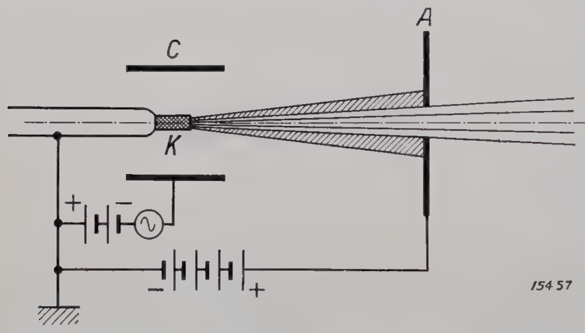

Fig. 2. Current modulation by modulation of the concentrating action of the Wehnelt cylinder.

Where the cathode beam is focussed by electromagnetic means, current modulation can be employed to similar purpose. The gradient of the helical paths described by the electrons [4]) is approximately equal to the distance between the cathode and anode and for control purposes is altered in synchronism with modulation. The cathode image thus alters its distance from the screen aperture so that a variable portion of the beam passes through the aperture.

### Current Modulation by means of the Space Charge

If the cylinder *C* (fig. 2) has a negative bias with respect to the cathode, a very powerful negative space charge is produced in the cathode space. Since the majority of the electrical lines of force pass between the anode and the highly-negative cylinder and practically no lines of force penetrate the interior of the cathode space, it is very difficult for the electrons to leave the cathode. On altering the potential of the cylinder, the current intensity is altered without a screen being required at all. The Wehnelt cylinder, which was originally used for the purpose of promoting spontaneous focussing in gasfilled tubes, here serves an altogether different purpose, and when used as such it will be referred to below as the control cylinder.

According to the magnitude of the negative bias of the control cylinder, more or less electrons will be able to leave their storage chamber, the cathode space. If the temperature of the cathode is sufficiently high to cause the continuous emission of excess electrons, it will not affect the intensity of the cathode ray, which is determined solely by the voltages of the control cylinder and the anode.

The storage chamber of the electrons can be regarded as a condenser of specific capacity. In other words, the charge accumulated in it, and hence also the charge density, is proportional to the potential $V$ applied to it. The intensity of the current flowing out of the storage chamber is proportional to the product of the charge density and the velocity of the electrons. As the charge density increases in proportion to the potential, and the velocity is proportional to the square root of the potential, the current intensity as long as it is determined by the space charge alone is proportional to $V^{3/2}$. The current-voltage curves of cathode ray tubes reproduced in fig. 5 show in fact that the current increases according to the 3/2 power of the control voltage.

The control cylinder of high-vacuum cathode-ray tubes serves the same purpose as the control grid in wireless valves. The control electrode is a cylinder closed at the front, which surrounds the cathode. The front wall is situated very close in front of the emitting surface of the cathode and has a small aperture at the centre. The current intensity of the cathode ray is determined not only by the control voltage, but also by the surface area of that part of the cathode participating in emission. In *fig. 3* the variation of the electric field between the cathode and the control electrode is represented diagrammatically. The greater the opposing voltage of the control electrode, the smaller will be the effective area of the cathode, which in fig. 3 is bounded by the points *a* and *b*. At the highest permissible currents of about 100 μA the diameter of the emitting surface is about 0.5 mm. With a diameter of 0.1 mm the electron current is only 1 μA.

---

[4]) Philips techn. Rev. **1**, 36, 1936.

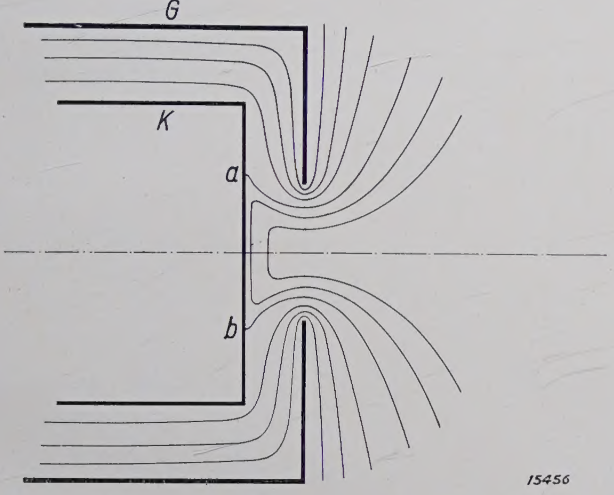

Fig. 3. Current modulation by means of a control electrode *G* placed very close to the surface of the cathode *K*. Diagrammatic sketch of the field with a cold cathode.

Only that portion of the emitting surface of the cathode between *a* and *b* participates in generating the cathode ray, as here the field applied at the cathode accelerates the electrons. Beyond the boundary points *a* and *b* the electrons are retarded by the external field and driven back to the cathode. The greater the negative potential applied to the control cylinder, the smaller becomes the distance between *a* and *b*. Finally *a* and *b* will coincide along the central line so that the portion of the cathode surface contributing to emission will become zero.

The arrangement of the electrodes in a Philips cathode ray tube designed for television purposes is shown in *fig. 4*. In addition to the negative control electrode $G_1$, these tubes are also provided with a positive screen-grid $G_2$, which screens off the fields of the electronic lenses $A_1$ and $A_2$ against the variable field of the control electrode. In the arrangement illustrated here potentials of about 10 volts are sufficient to control the electron beam intensity over a wide range. These small modulation potentials have practically no influence on the paths of the electrons, so that the definition of the fluorescent spot remains unaltered. The high sensitivity of this arrangement is due to its very compact construction from small components. A construction of this type requires a very homogeneous cathode material and an exact centring of the individual components.

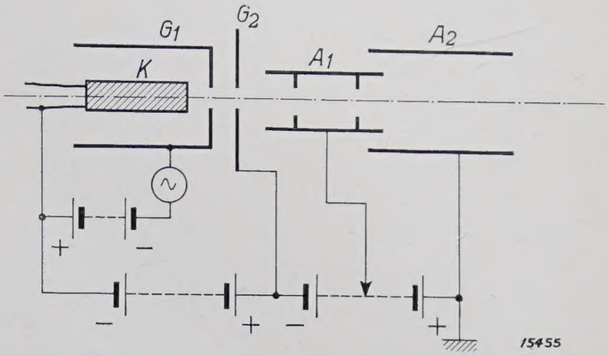

Fig. 4. Circuit diagram of a Philips cathode ray tube for television purposes.
$G_1$ = Control electrode. $G_2$ = Screen grid. $A_1$ and $A_2$ are anodes which serve for both the acceleration of the electrons and electron-optical focussing.

**Current-Voltage Curves of Intensity Modulation**

In order to gain some idea of what can be achieved by current modulation, it is necessary to know for each anode potential $V_a$ how the current $I_a$ varies with the potential $V_g$ of the control electrode. In this direction the arrangement corresponds completely to a radio valve equipped with a control grid. Accordingly the slope of the curve in which $I_a$ is plotted against $V_g$ may be taken as the gradient $S$ of the characteristic.

As indicated above, the anode current may be regarded as a function of a control potential $V$ applied to the supply chamber, which is principally determined by the potential $V_g$ of the control cylinder, although the anode potential also has a subsidiary influence, thus:

$$V = V_g + \frac{1}{g} V_a \quad . \; . \; . \; . \; . \quad (1)$$

$$\text{and } I_a = f(V) = f\left(V_g + \frac{1}{g} V_a\right) \quad . \; . \quad (2)$$

The amplification factor $g$ indicates to how much larger extent the potential $V_g$ of the control cylinder determines the anode current than the anode potential $V_a$ does. Equation (2) brings out the fact that the ratio $g$ of the effects produced by the potentials of the control electrode and the anode is independent of $V_a$ and $V_g$. This equation is useful if the characteristics $I_a = f(V_g)$ produced at different potentials $V_a$ can be brought to coincide by displacement in the direction of the $V_g$-axis. The ratio of the difference $\Delta V_a$ of the anode potentials of the two curves to the displacement $\Delta V_g$ is then the amplication factor $g$.

The characteristics of Philips 3951 and 3952 high-vacuum cathode-ray tubes for potentials of 1000 and 2000 volts at the anode $A_2$ (anode $A_1$ is at a potential of 200 and 400 volts respectively) are shown in *fig. 5*. It is observed that the curves have an almost uniform displacement of about 10 volts in the direction of the $V_g$-axis. The amplification factor of the tubes is thus $g = \Delta V_a / \Delta_g V = 1000/10 = 100$. With an anode potential of 1000 volts, the anode current can be regulated between 0 and 150 μA by altering the potential of the control cylinder between —25 volts and zero. With an anode potential of 2000 volts, the anode current can be regulated between zero and almost 30 μA. The modulation potential in this case must be varied between —35 volts and zero. The heating current is about 1 amp. The capacity of the control cylinder with respect to the other electrodes is 10 μμF.

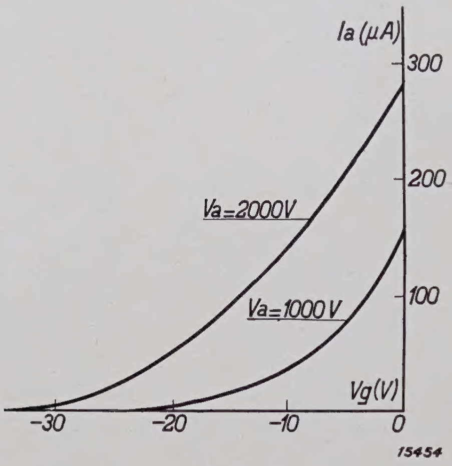

Fig. 5. Current-voltage curves for the Philips 3951 and 3952 cathode-ray tubes for anode potentials of 1000 and 2000 volts.

## Voltage Modulation

As stated at the outset, the intrinsic brilliance of the spot can also be controlled when keeping the current intensity constant, viz, by modulating the voltage of the fluorescent screen. A great disadvantage of voltage modulation is that the faster electrons are less influenced by the deflecting system than the slower ones. This may be avoided by stretching a large wire gauze directly in front of the screen and imparting to it a fixed potential difference as against the other electrodes, while the control voltage is applied between the wire gauze and the fluorescent screen (*fig. 6*). If the field of the screen has only a slight through-pull across the wire gauze, the deflection of the electrons is independent of the velocity with which they arrive at the pick-up screen.

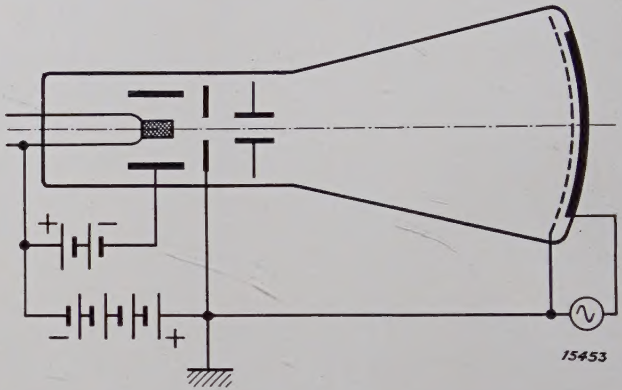

Fig. 6. Voltage modulation with a wire gauze placed in front of the pick-up screen.

However, every type of voltage modulation has the inherent disadvantage that, in order to obtain a sufficiently high control of the luminous intensity, control potentials of several thousand volts are required, while with current modulation potentials of the order of 10 volts are adequate.

Compiled by G. P. ITTMANN.

# PRACTICAL APPLICATIONS OF X-RAYS FOR THE EXAMINATION OF MATERIALS

## III.

By W. G. BURGERS.

The following example of X-ray analysis is of the same type as the two applications, Nos. 3 and 4, described in the previous part (II) of this section. Here again the preparations investigated differ only in texture, i.e. in the arrangement of the crystallites, and not in their chemical composition.

### 5. Texture of Electrolytically-Deposited Nickel Coatings

Electrolytically-deposited metal coatings may differ in many properties such as lustre, hardness, internal stresses, etc., according to the conditions of deposition employed, e.g. the composition of the plating bath, the current density, etc.

X-ray examination shows that in certain cases an alteration in the conditions of electrolysis may result in an alteration of the texture of the deposited coatings. Moreover, one and the same coating may be built up of zones with a different texture[1]).

*Fig. 1* reproduces an X-ray photograph of a nickel coating, 15 μ in thickness and having a metallic lustre, which was deposited on a copper rod in an industrial nickel plating bath. From the fairly uniform blackening on the whole circumference of the interference rings it may be deduced that the crystallites in the nickel coating are haphazardly positioned.

*Fig. 2a* is a photograph of a much thicker coating (150 μ) which has a matt surface. This picture reveals very marked intensity maxima round the periphery of the rings. The crystallites must therefore, at least in the outer zone of the nickel coating, possess a perfectly well-defined orientation. *Figs. 2b-d* are photographs of the same coating after etching to various depths. It is seen that the blackening of the rings becomes more and more uniform: in fig. 2d nearly the same picture is obtained as shown in fig. 1. The layer deposited first thus had no well-defined texture at all, the texture only having been developed as the coating was built up.

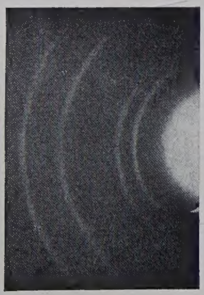

Fig. 1.

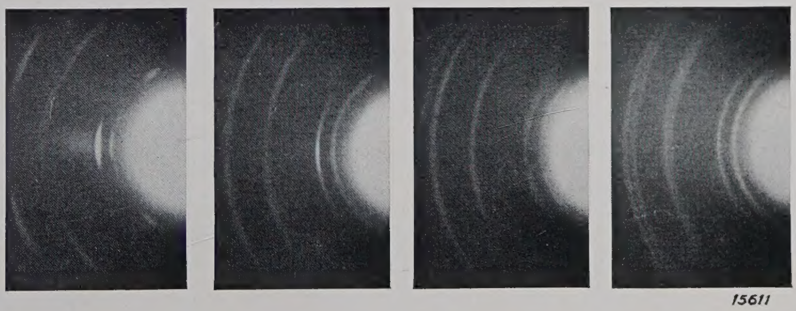

Fig. 2 a) b) c) d)

Fig. 1. X-ray photograph of an electrolytically-deposited nickel coating, 15 μ in thickness, possessing a metallic lustre.
Fig. 2. Zonal structure of an electrolytically-deposited nickel coating, 150 μ in thickness, with a matt surface.
a) The surface.
b)—d) After etching to depths of 100, 130 and 140 μ.
These photographs have been obtained by radiation grazing the nickel surface[2]). In fig. 2d the nickel coating is so thin that the interference lines of the substratum of copper also commence to become visible.

---

[1]) W. G. Burgers and W. Elenbaas, Naturwiss. **21**, 465, 1933.

[2]) Cf. fig. 4 in this section, part I, Philips Techn. Rev. **1**, 31, 1936.

# ABSTRACTS OF RECENT SCIENTIFIC PUBLICATIONS OF THE N.V. PHILIPS' GLOEILAMPENFABRIEKEN

**No. 1046:** P. J. Bouma: Verblinding (Polytechn. Wbl. **29**, 625-629, Oct. 1935).

A distinction is drawn between direct and indirect glare according as the rays producing glare do or do not fall on those parts of the retina whose reduction in sensitivity is observed. Furthermore a distinction is also made between simultaneous and successive glare. The former is a reduction in sensitivity during exposure to glare, and the latter that persisting some time after exposure. In this paper the effect of glare on the contrast sensitivity is investigated in relation to the position, dimensions, brightness and colour of the light-source. In general the results of the measurements made agree with those of Holladay; some small discrepancies appearing are discussed. A comparison is made between the glare effect with uniocular and binocular vision, and the question is studied how exposure to glare of one eye reacts on the contrast sensitivity of the other eye. Finally the author describes further measurements of the velocity with which the contrast sensitivity is restored, and measurements of the time during which white, sodium and mercury-vapour light continue to produce after-images on the yellow spot of the retina. (We shall revert to this subject in a subsequent issue of this Review).

**No. 1047:** W. Uyterhoeven and C. Verburg: Effets de la variation périodique de la concentration des atomes neutres de la vapeur dans une lampe à courant alternatif au sodium (C. R. Acad. Sci., Paris, **201**, 647-649, Oct. 1935).

For a 50-cycle alternating-current sodium lamp, oscillograms are obtained of the current, voltage and intensity of the yellow sodium light. The current varies almost sinusoidally, while the fluctuations of voltage and luminous intensity are on the other hand much more irregular. This is ascribed to the variable degree of ionisation of the sodium and the finite time separating ionisation, recombination at the walls and vaporisation. Actually the phase displacement between the current and the intensity maxima increases at higher frequencies. At a constant temperature the distortion of the voltage and intensity curves become still more marked if the current density is increased. The distortion is reduced if, at constant current, the temperature, and hence also the pressure of the sodium vapour, are raised. The intensity distribution in the sodium lines was found to be dependent on the time to some extent, as was to be expected from the periodic variation in concentration of the neutral sodium atoms.

**No. 1048*:** J. L. Snoek: Apparaat ter demonstratie van het ontstaan van ferromagnetische hysteresis (Faraday **5**, 141-144, May 1935).

Becker's theory of ferromagnetic hysteresis is illustrated by means of a mechanical model. A revolving arrow, which represents the direction of magnetisation, is positively connected to a tube ellipsoidally bent to give a total enclosure which is partly filled with mercury. The equilibrium positions of this tube represent the states with minimum magnetic energy. If in a magnetic material the preferred direction of magnetisation is everywhere the same and if an external magnetic field is applied perpendicular to this preferred direction, no hysteresis losses occur. Magnetisation is reversible, which can also be shown by the mechanical model.

**No. 1049:** W. G. Burgers and J. J. A. Ploos van Amstel: Cinematographic record of the $\alpha \rightleftarrows \gamma$ iron transition as seen by the electron-microscope (Nature, **136**, 721, Nov. 1935).

By careful volatilisation of barium and strontium oxides, the authors have succeeded in increasing the emission of electrons from an iron lamella to such an extent that emission was already sufficient at the transition temperature of about 900 deg. C to permit the recrystallisation process to be followed with the electron-microscope. On raising the temperature slowly above the transition point, it is possible to obtain complete recrystallisation in 5 to 10 mins. During this period an exposure of the electronic image was made every 4 secs. In this way a microfilm has been obtained which shows distinctly the growth of the $\alpha$-crystals in the $\gamma$-phase and the inverse.

---

*) A sufficient number of reprints for purposes of distribution is not available of those publications marked with an asterisk (*). Reprints of other publications may on application be obtained from Philips Laboratory, Kastanjelaan, Eindhoven, Holland.